

1 Discrete-Time Networks

1.0 Introduction

To realize a discrete-time filter with either computer software, a programmable DSP chip, or custom VLSI, a network must be specified describing the computations to be performed. For software realizations, the network corresponds to a flowchart of the filter algorithm, while for hardware realizations, the network describes the actual circuit elements and their interconnection. Many important properties of the discrete-time filter are placed in evidence by the coefficients of certain network structures. Significant computational savings can also be achieved in many cases by the proper choice of the network. And finally, the performance of a digital implementation is affected very substantially by the choice of the network structure because of the quantization effects we will study in chapter 11.

1.1 Flow Graph Properties

At least one implementation of a discrete-time filter is usually obvious from the form of its system function $H(z)$, and many others are readily generated, as we will see. Conversely, the system function $H(z)$ is readily deduced, in most cases, from a block diagram of some implementation of the filter.

The simple synthesis and analysis procedures described above for discrete-time networks are based on the following properties of linear flow graphs:

**Parallel
Networks**

We saw in (??) that if two filters or filter elements with impulse responses $h_1(n)$ and $h_2(n)$ are placed in parallel, the impulse response $h(n)$ of the combination equals $h_1(n) + h_2(n)$. Hence, the system function of the parallel network is given by

$$H(z) = H_1(z) + H_2(z). \quad (1.1.1)$$

**Cascade
Networks**

If two filters or filter elements are placed in cascade, then from (??) we have $h(n) = h_1(n) * h_2(n)$, and thus the system function of the cascade network is simply

$$H(z) = H_1(z)H_2(z). \quad (1.1.2)$$

**Feedback
Networks**

If three filter elements with individual system functions $E(z)$, $F(z)$, and $G(z)$ are arranged in the positive feedback configuration of figure 1.1, the overall system function of the feedback network is given by

$$H(z) = \frac{E(z)F(z)}{1 - F(z)G(z)}. \quad (1.1.3)$$

This is readily derived by relating $X(z)$, $Y(z)$, and $W(z)$, and is directly analogous to the corresponding Laplace transform property for continuous-time networks. In words, “the system function equals the feedforward transfer function divided by one minus the loop transfer function”. (See problem 5.1.)

EXAMPLE

As an example of the ease with which the above properties can usually be employed to obtain the system function from a block diagram of the filter, consider the discrete-time network of figure ???. This network is

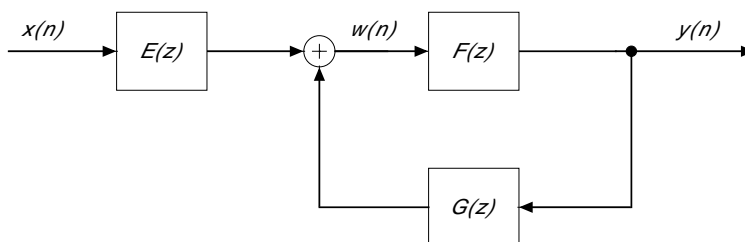


Figure 1.1: A general feedback configuration.

readily identified as being of the general form shown in figure 5.1 by using the preceding parallel and cascade network properties to show that

$$E(z) = \sum_{m=0}^M b_m z^{-m}, \quad F(z) = 1, \quad G(z) = - \sum_{k=1}^N a_k z^{-k}. \quad (1.1.4)$$

But then, from (1.1.3), we have immediately that

$$H(z) = \frac{\sum_{m=0}^M b_m z^{-m}}{1 + \sum_{k=1}^N a_k z^{-k}} \quad (1.1.5)$$

which is the same as (??) since $a_0 = 1$ in the difference equation that originally led to this network.

Note also that since $z^{-1}\mathbf{A}$ is the loop gain of the network in state-variable form in figure ??, we can interpret (??) as being a generalization of (1.1.3) to include vector signals. In this case, however, we must take care to order the vectors and matrices correctly as in (??).

EXAMPLE

We will find the system function for the interconnection of sub-systems shown on following page. Note first that the transfer function $H(z)$ from $x(n)$ to $w(n)$ is simply

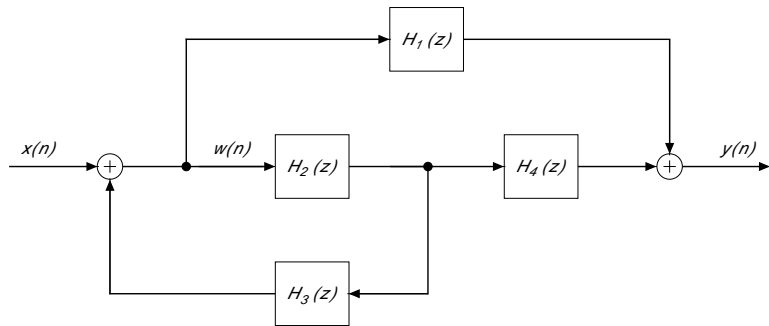
$$H_w(z) = \frac{W(z)}{X(z)} = \frac{1}{1 - H_2(z)H_3(z)}$$

because the feedforward transfer function to $w(n)$ is unity and the loop transfer function is the cascade of $H_2(z)$ and $H_3(z)$. Then, there are two parallel paths from $w(n)$ to $y(n)$ with transfer functions of $H_1(z)$ and $H_2(z)H_4(z)$, respectively. Therefore,

$$Y(z) = W(z)[H_1(z) + H_2(z)H_4(z)]$$

and

$$H(z) = \frac{W(z) Y(z)}{X(z) W(z)} = \frac{H_1(z) + H_2(z)H_4(z)}{1 - H_2(z)H_3(z)}.$$



Another interesting and useful network property is that pertaining to *transpose* networks.

Transpose Networks

If the directions of all branches in the flow graph for a discrete-time filter are reversed, the system function of the resulting *transpose* network is the same as that of the original network. The input and output of the transpose network correspond, respectively, to the output and input of the original network. All *branch nodes* in the original network become *summation nodes* in the transpose network, and likewise summation nodes become branch nodes. This is illustrated in figure 1.2 for a second-order filter. The fact that the system function is unchanged by transposition can be proved using several approaches including Tellegen's theorem for discrete-time networks, Mason's rule for transfer function evaluation, or

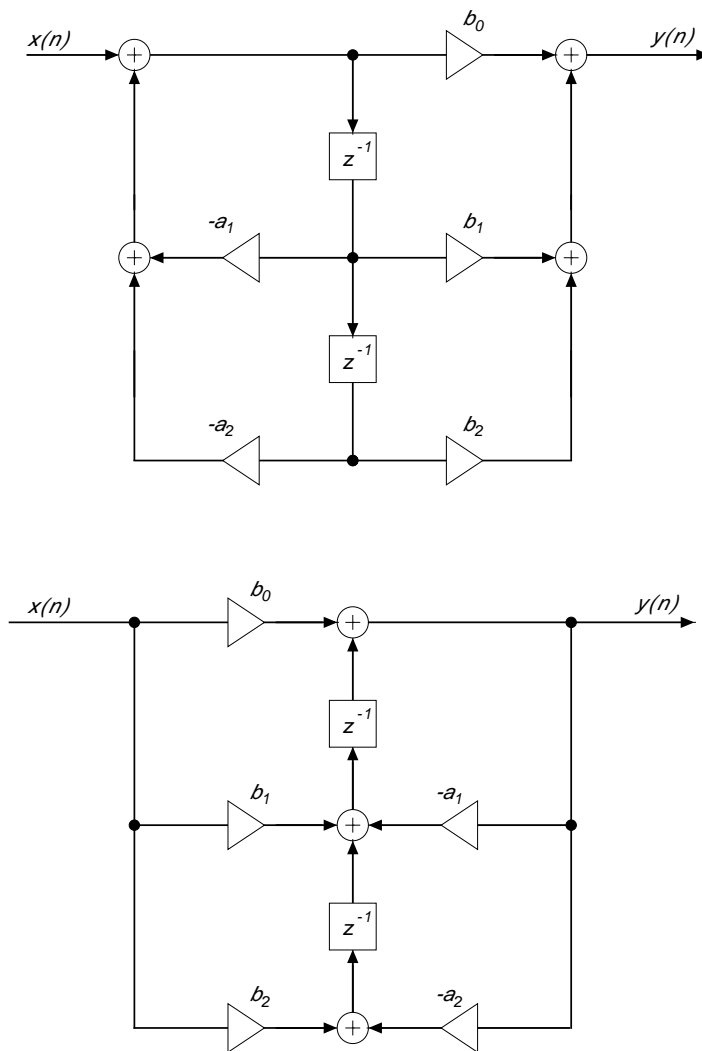


Figure 1.2: Transpose second-order networks.

a state-variable formulation. We will use the last method to prove this result, as follows: Reversing the branch directions of a network in state-variable form as depicted in figure ??, we produce the state-variable description of the transpose network shown in figure 1.3. Note that \underline{c} replaces \underline{b} and \underline{b}^t replaces \underline{c}^t . To see that \mathbf{A}^t replaces \mathbf{A} , as indicated, note that the gain a_{ij} from $s_j(n)$ to $s_i(n+1)$ becomes the gain from $s_i(n)$ to $s_j(n+1)$ in the transpose network. Hence, a_{ji} must replace a_{ij} . The system function for the transpose network is, therefore,

$$H^t(z) = d + z^{-1}\underline{b}^t(\mathbf{I} - z^{-1}\mathbf{A}^t)^{-1}\underline{c}. \quad (1.1.6)$$

But this is just the matrix transpose of the 1×1 “matrix” $H(z)$, and thus $H(z) = H^t(z)$, which proves the assertion.

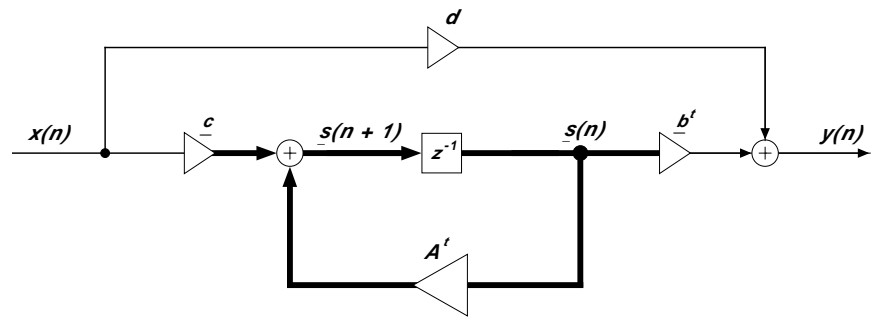


Figure 1.3: Transpose of the state-variable description in figure ??.

Although $H(z)$ and its associated output $y(n)$ are unchanged by transposition, the state vectors $\underline{s}(n)$ and $\underline{\hat{s}}(n)$ before and after transposition will be quite different, in general, and this is one of the tools we can use to modify and/or optimize the structure and performance of a digital filter.

1.2 Network Structures

The variety of possible structures for discrete-time networks is extremely wide and diverse, and the question of optimal digital-filter structures has attracted great research interest. The term *digital filter* is used above in conjunction with optimal structures because it is only when the effects of quantization are considered that significant differences arise in the performance of different network structures. Therefore, we will defer most of our comparative analysis of network structures until quantization effects are studied in chapter 11, but the most common structures and their basic properties will be introduced in this section.

Direct Form

The structure previously shown in figure ?? is often called the *direct form* of a discrete-time filter because it is a direct implementation of the basic difference equation in (??). However, in the case of IIR filters, a more efficient structure in the sense of fewer delays can be generated by reversing the order of the two filter sections, which are effectively in cascade. That is, letting

$$H_1(z) = N(z) = \sum_{m=0}^M b_m z^{-m}$$

and

$$H_2(z) = \frac{1}{D(z)} = \frac{1}{\sum_{k=0}^N a_k z^{-k}} \quad (1.2.1)$$

where $a_0 = 1$, figure ?? realizes the system function $H(z) = H_1(z)H_2(z)$ with $H_1(z)$ first, followed by $H_2(z)$. Reversing this order and eliminating the $\min(N, M)$ delays that are thereby made redundant, we obtain the structure shown in figure 1.4 for $M = N$, which we will call *direct form II*.

Although direct form II still satisfies the difference equation in (??), it does not implement this difference equation directly. Rather, it is a direct implementation of a pair of equations relating $x(n)$, $y(n)$, and $w(n)$, as follows:

$$w(n) = x(n) - \sum_{k=1}^N a_k w(n-k)$$

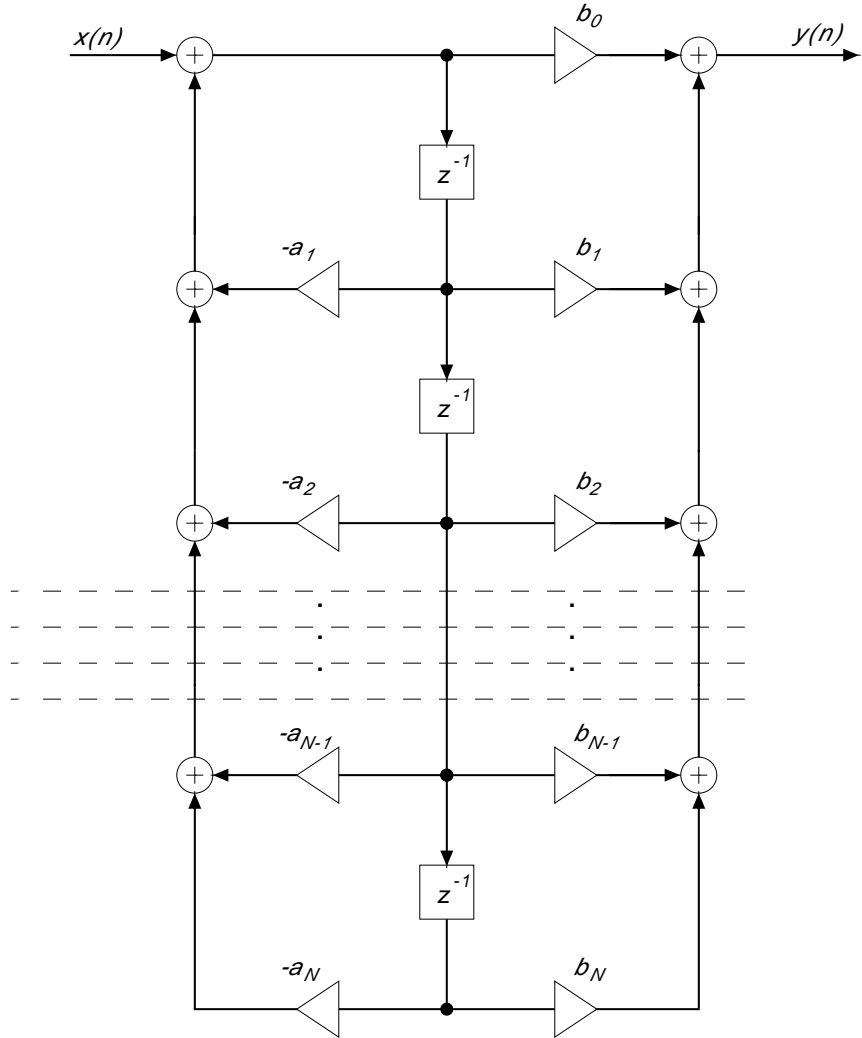


Figure 1.4: Direct-form-II structure.

$$y(n) = \sum_{m=0}^M b_m w(n-m). \quad (1.2.2)$$

Note that this structure is still recursive, but in the intermediate output $w(n)$ and not the final output $y(n)$.

The transpose network corresponding to direct form II, which we will call direct form I, is shown in figure 1.5. Since the order of $H_1(z)$ and $H_2(z)$ is reversed again by transposition in direct form I, this form is quite similar to the original direct form in figure ???. However, up to half of the delays have been eliminated by moving their location in the network structure.

Direct forms I and II are examples of *canonical* structures in that, in general, they realize the given system function with the smallest possible numbers of delays, adders, and multipliers. Assuming $M = N$, as is often the case for IIR filters, the number of each of these components required in a canonical implementation is as follows:

$$\begin{aligned} \text{number of delays} &= N, \\ \text{number of adders} &= 2N, \\ \text{number of multipliers} &= 2N + 1. \end{aligned} \quad (1.2.3)$$

By *adders* we mean two-input adders, and thus a summation node with \mathcal{J} inputs implies $\mathcal{J} - 1$ adders in the implementation. The reader can check that (1.2.3) is indeed satisfied by direct forms I and II when $M = N$.

Parallel Form

The expansion of $H(z)$ in a partial-fraction expansion leads to another pair of canonical structures called the *parallel forms*. In order to produce real multiplier coefficients in the filter structure, the terms in the partial-fraction expansion corresponding to complex-conjugate pole pairs must be combined into second-order terms; and it is convenient for both notation and implementation reasons to combine the real poles in pairs as well. We thereby produce the following form of the system function,

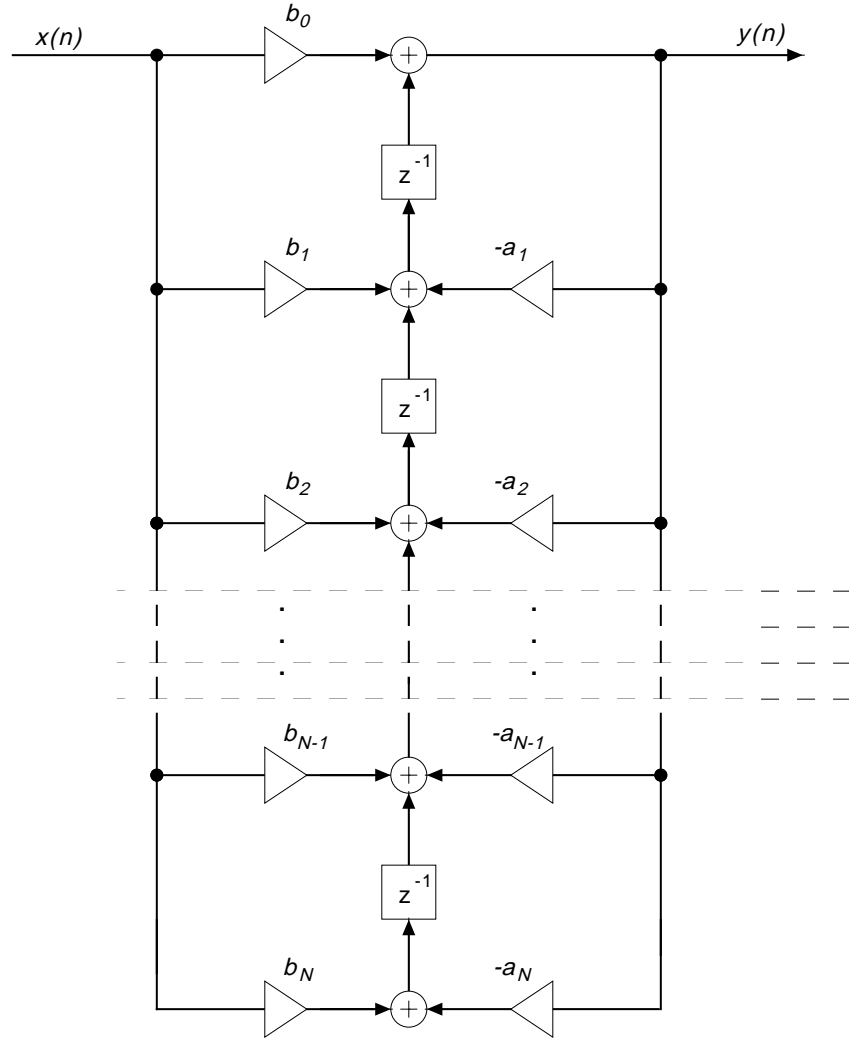


Figure 1.5: Direct-from-I structure.

assuming again that $M = N$:

$$\begin{aligned} H(z) &= \gamma_0 + \sum_{k=1}^N \frac{A_k}{1 - p_k z^{-1}} \\ &= \gamma_0 + \sum_{i=1}^L \frac{\gamma_{0i} + \gamma_{1i} z^{-1}}{1 + \alpha_{1i} z^{-1} + \alpha_{2i} z^{-2}} \end{aligned} \quad (1.2.4)$$

with

$$L = \left[\frac{N+1}{2} \right]_{int}, \quad (1.2.5)$$

where $[]_{int}$ denotes the *integer part of*. If N is odd, there is one first-order term in (1.2.4), say for $i = L$, and we then have $\gamma_{1L} = \alpha_{2L} = 0$. We will investigate additional properties of these filter coefficients in the next section. Equation (??) corresponds to a similar, but different parallel structure.

Since the system function in (1.2.4) is expressed as a sum of second-order terms, the corresponding implementations must consist of parallel combinations of second-order networks or *sections*. Realizing each section as a direct-form-II network, we obtain *parallel form II*, which is shown in figure 1.6. Alternatively, we may employ direct form I networks for the second-order sections to produce *parallel form I*, shown in figure 1.7. Note that parallel forms I and II both satisfy (1.2.3) (keeping in mind that one section is first-order if N is odd), and hence these are also canonical forms. Moreover, note that parallel form II is, in fact, the transpose of parallel form I.

Cascade Form

If, in addition to factoring the denominator polynomial $D(z)$ in (1.2.1) into second-order factors as for the parallel forms, the numerator polynomial $N(z)$ is similarly factored, the system function can be written as the product

$$H(z) = b_0 \prod_{k=1}^N \frac{1 - z_k z^{-1}}{1 - p_k z^{-1}} = b_0 \prod_{i=1}^L H_i(z), \quad (1.2.6)$$

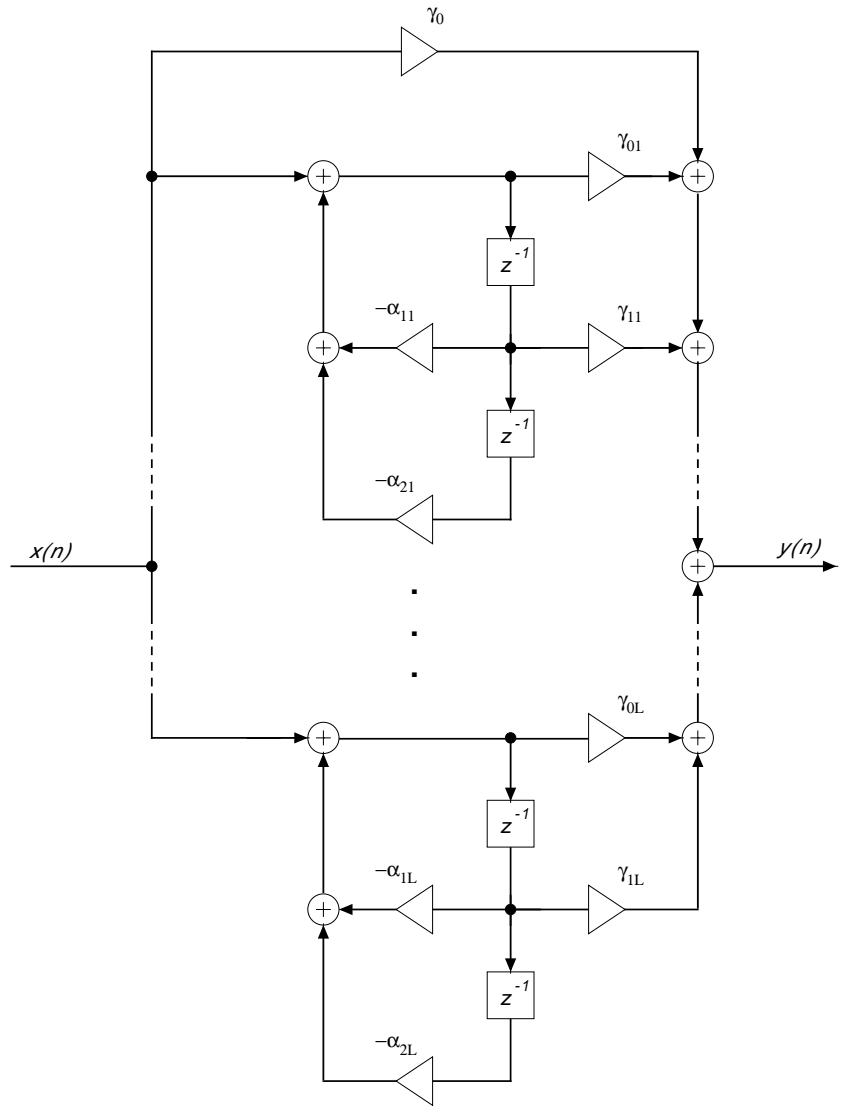


Figure 1.6: Parallel-from-II structure.

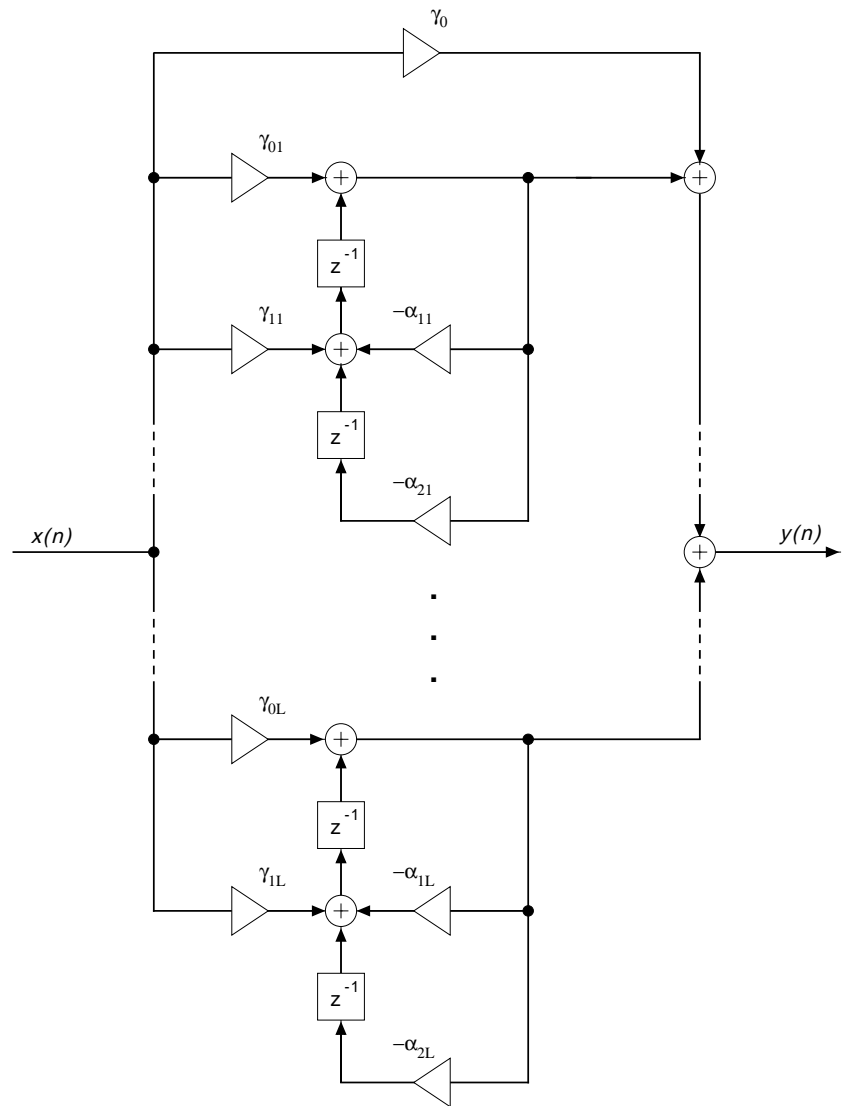


Figure 1.7: Parallel-from-I structure.

where

$$H_i(z) = \frac{1 + \beta_{1i}z^{-1} + \beta_{2i}z^{-2}}{1 + \alpha_{1i}z^{-1} + \alpha_{2i}z^{-2}}. \quad (1.2.7)$$

L is again given by (5.2.5), and $\alpha_{2L} = \beta_{2L} = 0$ if N is odd. Since $H(z)$ is formed as the product of the second-order functions $H_i(z)$, the corresponding filter structure must comprise a cascade of second-order sections. Implementing these sections in direct forms II and I, we produce *cascade forms II and I*, respectively, shown in figures 1.8 and 1.9. The reader can verify that these structures are also canonical and that they are related in topology by transposition. However, cascade form II is actually the transpose of form I only if the order of the filter sections is reversed from one form to the other.

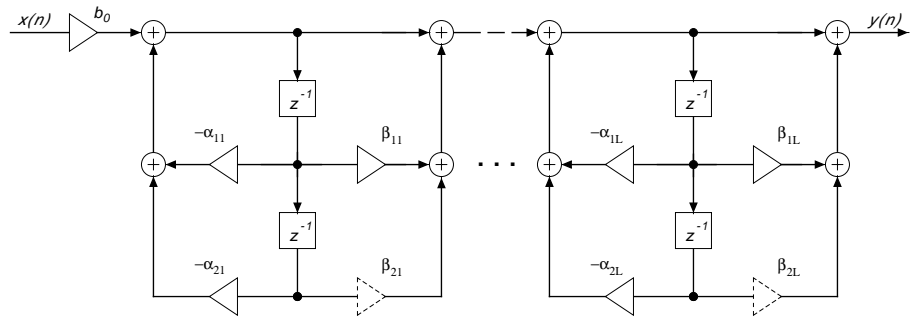


Figure 1.8: Cascade-from-II structure.

Many other filter structures can obviously be produced using, for example, combinations of the parallel and cascade forms, various feedback arrangements, continued-fraction expansions of $H(z)$, and so forth. Many additional structures can be generated as analogs of classical continuous-time filters and have names such as *wave digital filters*, *ladder structures*, and *lattice structures*. A complete description of all these structures is beyond the scope of this book, but several of them will be considered in

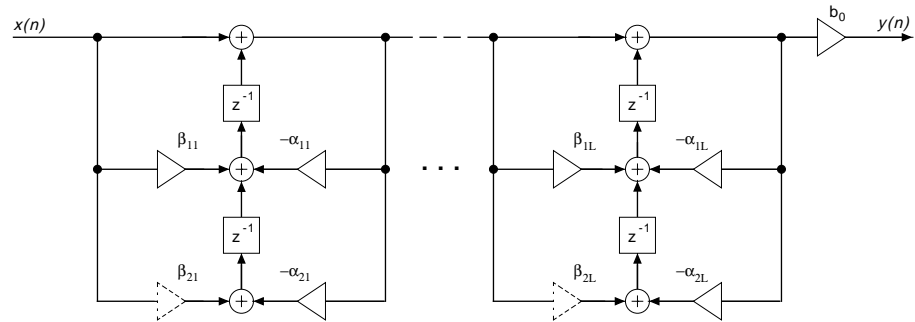


Figure 1.9: Cascade-from-I structure.

subsequent chapters. By far the most common digital-filter structures are the direct, parallel, and cascade forms; and of these, the cascade forms are most often employed for IIR filters for reasons concerning quantization and implementation. In the case of FIR filters, only the direct and cascade forms are applicable, with the direct form being most commonly employed.

We will often refer in the remainder of this book to simply the “direct form,” the “parallel form,” or the “cascade form,” although we have actually defined two network structures in each case. This is done for convenience in view of the fact that each pair of structures implements the same form of the system function $H(z)$. Thus, in effect, we refer by this terminology to the form of the system function itself as expressed in (1.1.5), (1.2.4), or (1.2.6).

MATLAB Exercise No. 7 - Cascade and Parallel Forms

Cascade and parallel structures for IIR filters are readily synthesized using the `zp2sos` or `ss2sos` commands in the MATLAB Signal Processing Toolbox. As a sample IIR design, we will use a fifth-order Chebyshev Type-2 lowpass filter with at least 30-dB stopband attenuation from 0.2π to π (i.e., from 0.2 to 1.0 on the normalized frequency scale in MATLAB).

(IIR filter designs are covered in chapter 8.) That is, let

$$[z,p,k] = \text{cheby2}(5,30,0.2)$$

Note that the resulting zeros and poles are either real or occur in complex-conjugate pairs, as expected. Use `zplane` to draw the pole/zero diagram. To convert the zeros (`z`), poles (`p`), and gain (`k`) to direct-form coefficients, type

$$[b,a] = \text{zp2tf}(z,p,k)$$

or use

$$\begin{aligned} b &= k * \text{poly}(z) \\ a &= \text{poly}(p) \end{aligned}$$

Plot the associated magnitude (Bode) response to check the frequency range of the stopband and its attenuation. The conversion from *zero-pole-to-second-order-sections* (i.e., cascade form) is then provided by

$$\text{cas} = \text{zp2sos}(z,p,k)$$

Do the columns of `cas` (section coefficients) have the expected form for zeros on the unit circle and stable poles? (See `help`.) Produce a magnitude plot for each section, for sections 1 and 2 in cascade, and for all three in cascade. (Individual columns are designated by `cas(:,2)` for the second column, etc. Use element-by-element products of the section magnitude responses, or simply sums in dB.) Note that the cascaded section responses (1, 1 – 2, and 1 – 2 – 3) are scaled to unity or less to prevent overflow in a fixed-point implementation of the cascade-form-I filter. A parallel form can also be obtained from the partial-fraction expansion of $H(z)$, that is,

$$[r,p,d] = \text{residuez}(b,a)$$

However, this corresponds to a parallel form of first-order sections having complex coefficients, in general. Figure out how to combine these first-order complex terms into second-order sections with real-valued coefficients, and do this to produce the standard parallel form. Generate the frequency response for each section, and combine them appropriately to produce the overall frequency response.

1.3 Properties of Network Coefficients

One can quickly determine a number of important properties of a discrete-time filter from the coefficients of certain network structures. In the case of IIR filters, information concerning such things as stability, real or complex singularities, transmission zeros, and quantization effects is readily obtained from the cascade-form coefficients or, to a lesser extent, the parallel-form coefficients. For FIR filters, such properties as linear phase, 90° phase shift, or symmetrical frequency response are apparent from the coefficients of the direct form or certain cascade structures.

The denominator factors of the parallel and cascade forms and the numerator factors of the cascade form are all quadratic functions of the form

$$\begin{aligned} F_i(z) &= 1 + c_{1i}z^{-1} + c_{2i}z^{-2} \\ &= (1 - q_{1i}z^{-1})(1 - q_{2i}z^{-1}) \end{aligned} \quad (1.3.1)$$

where the roots q_{1i} and q_{2i} are the corresponding singularity (pole or zero) locations in the z plane. The roots may be real or complex, but in either case

$$c_{1i} = -(q_{1i} + q_{2i}), \quad (1.3.2)$$

$$c_{2i} = q_{1i}q_{2i}. \quad (1.3.3)$$

If $c_{1i}^2 \geq 4c_{2i}$, the roots are real, while if $c_{1i}^2 < 4c_{2i}$, the roots are complex conjugates. Letting $q_{1i} = q_{2i}^* = q_i$ in the latter case, we have

$$c_{1i} = -2 \operatorname{Re}(q_i) = -2r_i \cos \theta_i, \quad (1.3.4)$$

$$c_{2i} = |q_i|^2 = r_i^2, \quad (1.3.5)$$

where r_i is the radius of the singularities in the z plane, and $\pm\theta_i$ are the corresponding angles. Therefore, the pole locations are quickly calculated from the coefficients of the parallel or cascade forms, and for the cascade form, the zeros are similarly determined.

Stability

As a result of the above, we can readily obtain conditions on the coefficients of the parallel or cascade forms to ensure the stability of the filter. Specifically, the second-order denominator factors of these forms are given by

$$\begin{aligned} D_i(z) &= 1 + \alpha_{1i}z^{-1} + \alpha_{2i}z^{-2} \\ &= (1 - p_{1i}z^{-1})(1 - p_{2i}z^{-1}) \end{aligned}$$

and the poles must lie inside the unit circle for stability, i.e.,

$$|p_{1i}|, |p_{2i}| < 1.$$

Hence, from (1.3.3),

$$|\alpha_{2i}| = |p_{1i}p_{2i}| < 1. \quad (1.3.6)$$

The corresponding condition on α_{1i} is obtained from the expression

$$p_{1i}, p_{2i} = \frac{-\alpha_{1i} \pm \sqrt{\alpha_{1i}^2 - 4\alpha_{2i}}}{2}$$

and is given by (see problem 5.4)

$$|\alpha_{1i}| < 1 + \alpha_{2i}. \quad (1.3.7)$$

Conditions (1.3.6) and (1.3.7) are illustrated in figure 5.10, which shows the resulting stability triangle in the α_1, α_2 plane. That is, the second-order section is stable if, and only if, α_{1i} and α_{2i} define a point that lies inside this triangle. As previously noted, the poles are complex if $\alpha_1^2 < 4\alpha_2$, and real otherwise.

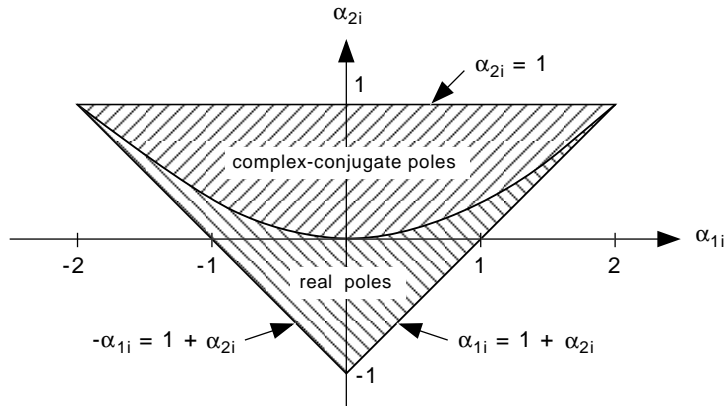


Figure 1.10: Region of coefficient values for which a second-order filter is stable.

Very often, the zeros of $H(z)$ lie on the unit circle in the z plane. In fact, as we will see in chapter 8, this is always true for discrete-time filters derived by bilinear transformation from the classical continuous-time designs. If these zeros are complex conjugates (including two equal real zeros), then from (1.3.5) we see that the numerator coefficients β_{2i} of the cascade form must be unity. So, in this case,

$$\beta_{1i} = -2 \cos \theta_i \quad \text{and} \quad \beta_{2i} = 1.$$

In particular, if the zeros are real and equal, we have

$$\beta_{1i} = \pm 2.$$

If a second-order section has unequal real zeros of unit magnitude, then they must be $z_{1i} = 1$ and $z_{2i} = -1$, and thus from (1.3.2) and (1.3.3),

$$\beta_{1i} = 0 \quad \text{and} \quad \beta_{2i} = -1.$$

If the numerator is actually first-order with only one zero, then of course

$$\beta_{1i} = \pm 1 \quad \text{and} \quad \beta_{2i} = 0.$$

Therefore, in all of the above cases of zeros on the unit circle, the β_{2i} coefficients of the cascade form are always the integers ± 1 or 0, and the β_{1i} are also integers ($\pm 2, \pm 1$, or 0) if the zeros are real. For this reason, the β_{2i} multipliers were shown with dotted lines in figures 1.8 and 1.9 because actual multipliers are not required to implement these integer coefficients. This, in part, explains the popularity of the cascade form with designers since 25% to as much as 50% of the multiplication time or hardware can be saved in filters having zeros on the unit circle.

EXAMPLE

To practice with the polar form in (1.3.4) and (1.3.5), we will find the poles and zeros for the cascade form

$$H(z) = \frac{(1 + 1.414z^{-1} + z^{-2})(1 + 2z^{-1} + z^{-2})}{(1 - 0.8z^{-1} + 0.64z^{-2})(1 - 1.08333z^{-1} + 0.25z^{-2})}$$

Since the numerator coefficients fall on the boundary of the stability triangle and the z^{-2} coefficients are unity, the radii of all the zeros must be unity. The coefficient $1.414 = -2 \cos \theta$ implies that $\cos \theta = -0.707$, and thus one pair of zeros lies on the unit circle at angles of $\pm 3\pi/4$. The other z^{-1} coefficient in the numerator is 2, and so the other pair of zeros both fall at $z = -1$. The first z^{-2} coefficient in the denominator is 0.64, and thus if these poles are complex, their radius is 0.8. The corresponding z^{-1} coefficient is $-0.8 = -2(0.8) \cos \theta$ or $\cos \theta = 0.5$, and hence one pair of poles is indeed a complex-conjugate pair with a radius of 0.8 and angles of $\pm \pi/3$. The final denominator factor has a z^{-2} coefficient of 0.25, and thus if these poles are complex, their radius is 0.5. However, $-1.08333 = -2(0.5) \cos \theta$ implies that $\cos \theta$ is greater than unity, which it cannot be. Therefore, these poles are actually real and equal 0.75 and 0.333, respectively.

Linear Phase

Turning to FIR filters, we will investigate what is perhaps their most important property, namely, that the *coefficients of an FIR filter are easily constrained to produce a linear phase response. The corresponding constraint is simply that the finite-duration impulse response have*

conjugate-even or conjugate-odd symmetry about its midpoint. To see that this constraint ensures linear phase, consider the FIR system function

$$H(z) = \sum_{m=0}^M b_m z^{-m} \quad (1.3.8)$$

with

$$b_m = \pm b_{M-m}^* = |b_m| e^{j\phi_m}.$$

If M is even, the coefficient $b_{M/2}$ is real and corresponds to the center of symmetry of $h(n)$, while if M is odd, there is no central coefficient. These four cases are illustrated in figure 1.11 for b_m real, where we then have

$$b_m = \pm b_{M-m}.$$

Note that type-I and -II filters have even symmetry about their midpoints, while type-III and -IV filters have odd symmetry. On the other hand, types I and III have even order (M), while types II and IV have odd order.

Considering the convolution of these real-valued impulse responses with a constant (dc) input or the Nyquist-frequency sequence $(-1)^n$, we observe that odd-symmetry implies zero output for all dc inputs, and hence $H(z)$ must have a zero at $z = 1$ for type-III and -IV filters. That is

$$\sum_{n=0}^M h(n) = H(1) = 0 \quad (\text{for types III and IV}).$$

Also, types II and III will have zero output for Nyquist-frequency inputs because

$$\sum_{n=0}^M (-1)^n h(n) = H(-1) = 0 \quad (\text{for types II and III}),$$

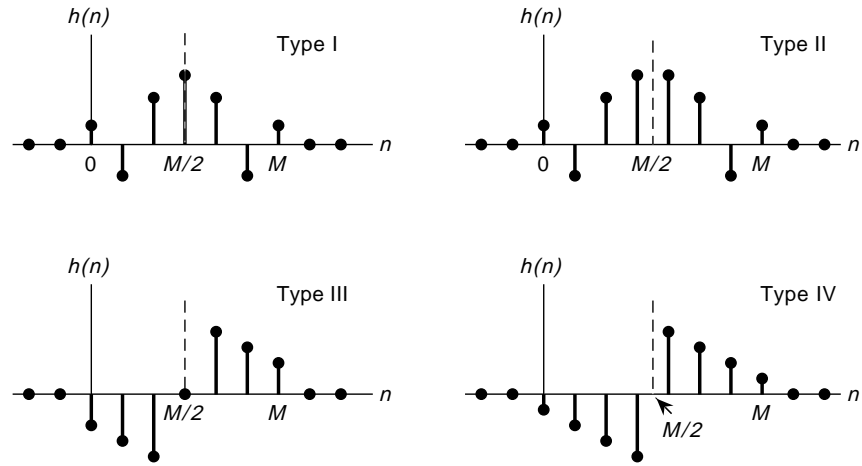


Figure 1.11: Four cases of even/order symmetry about $M/2$ for real-valued, linear-phase FIR filters with even or odd (M).

and thus $H(z)$ has a zero at $z = -1$. These constrained zeros at $z = \pm 1$ for real-valued linear-phase FIR filters are shown and marked by arrows on the corresponding z -plane plots in figure 1.12.

A further effect of the linear-phase constraint on the zeros of $H(z)$ is seen by noting from (1.3.8) that

$$z^M H(z) = \pm H^*(1/z^*) \tag{1.3.9}$$

because of the assumed symmetry in the b_m . Equation (1.3.9) implies that the zeros of $H(z)$ must also be zeros of $H^*(1/z^*)$, which means that if z_m is a zero of $H(z)$, then $1/z_m^*$ is also. Therefore, *the zeros of a linear-phase filter either must lie on the unit circle or must occur in pairs with reciprocal radii*. For b_m real, the zeros must also occur as complex conjugates; and thus in that case, those not lying on the unit circle or the real axis will actually occur in quadruples, as illustrated in figure 1.12.

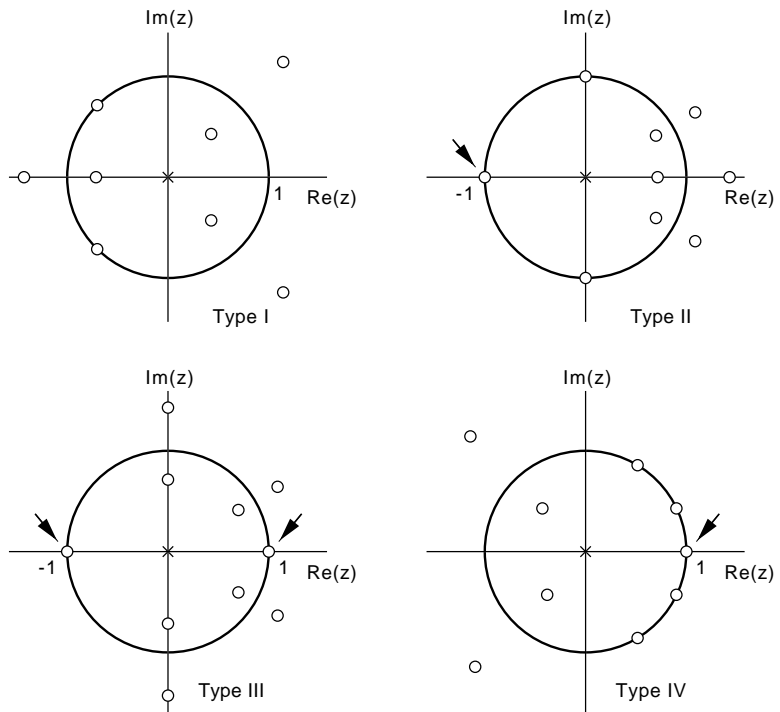


Figure 1.12: Typical Zeros locations for type-I, -II, -III, and -IV linear-phase FIR filters from figure 1.11 showing required zeros at $z = \pm 1$.

Type I

Considering first the type-I case of conjugate-even symmetry and M even, we may rewrite (1.3.8) as

$$\begin{aligned}
 H(z) &= z^{-M/2} \left[\sum_{m=0}^M b_m z^{-m+M/2} \right] \\
 &= z^{-M/2} \left[b_{M/2} + \sum_{m=0}^{M/2-1} (b_m z^{-m+M/2} + b_{M-m} z^{m-M/2}) \right].
 \end{aligned} \tag{1.3.10}$$

Substituting $z = e^{j\omega}$ and taking into account that $b_m^* = b_{M-m}$, we find that the frequency response is given by

$$\begin{aligned} H'(\omega) &= e^{-j\omega M/2} \left\{ b_{M/2} + \sum_{m=0}^{M/2-1} 2|b_m| \cos\left[\left(\frac{M}{2} - m\right)\omega + \phi_m\right] \right\} \\ &= e^{-j\omega M/2} R(\omega) \end{aligned} \quad (1.3.11)$$

where $R(\omega)$ is purely real. If $R(\omega)$ is of constant sign for all ω , then $R(\omega) = \pm |H'(\omega)|$ and we indeed have the linear phase response

$$\angle H'(\omega) = -\omega \frac{M}{2} + C$$

where $C = 0$ or π . If, however, there are sign changes in $R(\omega)$, there are corresponding 180° phase shifts in $\angle H'(\omega)$, and $\angle H'(\omega)$ is only piecewise linear. It is common practice, nonetheless, still to refer to the filter as having simply *linear phase*. This terminology is reasonable since we are actually trying to constrain the filter's *group delay* $D(\omega)$ to be constant, and since

$$D(\omega) = -\frac{d}{d\omega} \angle H'(\omega)$$

we have

$$D(\omega) = \frac{M}{2} \quad (1.3.12)$$

except at those frequencies where $R(\omega)$ changes sign. But at those frequencies, $R(\omega) = |H'(\omega)| = 0$, and hence there is no output contribution anyway. Hence, the group delay is simply the delay to the midpoint of $h(n)$ (see figure 1.11).

The implication of constant group delay is that all frequency components of an input sequence are similarly delayed in the output sequence. Hence, the symmetry (odd or even) of an input pulse sequence, for example, is preserved in the output sequence if the impulse response $h(n)$ has even symmetry. The delay between the corresponding centers of symmetry is just the group delay, and this corresponds to the delay in

$h(n)$ at its center of symmetry. For the above case of M even, the group delay equals an integer number of sampling periods and thus is easily accounted for in subsequent data processing.

Type II

The type-II case of M odd leads to expressions similar to (1.3.10) and (1.3.11), and equation (1.3.12) still holds for the group delay in this case. However, since this delay is no longer an integer number of sampling periods for odd M , it can be more difficult to account for unless we wish to interpolate between samples.

EXAMPLE Interpolator

A crude way to interpolate between adjacent samples of a signal $x(n)$ is simply to average each pair of adjacent samples, that is,

$$y(n) = \frac{1}{2}[x(n) + x(n-1)]$$

corresponding to the causal first-order type-II filter

$$h(n) = \frac{1}{2}[\delta(n) + \delta(n-1)].$$

The system function is thus

$$H(z) = \frac{1}{2}[1 + z^{-1}],$$

which has a single zero at $z = -1$ (as expected for even symmetry and M odd). The frequency response is

$$\begin{aligned} H'(\omega) &= \frac{1}{2}[1 + e^{-j\omega}] \\ &= \frac{1}{2}e^{-j\omega/2}[e^{j\omega/2} + e^{-j\omega/2}] \\ &= e^{-j\omega/2} \cos(\omega/2). \end{aligned}$$

Hence, the filter is indeed linear phase with a group delay of $1/2$. The real function $R(\omega)$ is the simple lowpass response

$$R(\omega) = \cos(\omega/2),$$

which falls off monotonically to zero at $\omega = \pi$. In general, interpolation filters are lowpass functions, as argued in section 13.1.

Types III and IV

Conjugate-odd symmetry in an FIR impulse response is also associated with an important class of discrete-time filters. These filters provide a 90° phase shift at all frequencies, in addition to constant group delay. This is seen by evaluating (1.3.10) for $z = e^{j\omega}$ and $b_{M-m} = -b_m^*$ to obtain

$$\begin{aligned} H'(\omega) &= e^{-j\omega M/2} \left\{ b_{M/2} + j \sum_{m=0}^{M/2-1} 2|b_m| \sin \left[\left(\frac{M}{2} - m \right) \omega + \phi_m \right] \right\} \\ &= j e^{-j\omega M/2} R(\omega) \end{aligned} \quad (1.3.13)$$

since $j = e^{j\pi/2}$ implies a phase shift of $\pi/2$. $R(\omega)$ is again real because $b_{M/2}$ is either purely imaginary (in the general case) or zero (in the real-valued case) to satisfy the symmetry condition. Such FIR filters are useful, for example, in approximating the ideal differentiator response

$$H'_D(\omega) = j\omega, \quad -\pi < \omega < \pi. \quad (1.3.14)$$

As indicated above, the factor j in $H'_D(\omega)$ is realized exactly by the symmetry condition, and we design the coefficients b_m so that $R(\omega)$ approximates

$$R(\omega) \approx \omega, \quad -\pi < \omega < \pi. \quad (1.3.15)$$

There is, of course, an additional linear-phase factor in (1.3.13), which can be eliminated for M even if the filter is made noncausal and is centered at $n = 0$. Another example is the ideal Hilbert transformer

$$H'_H(\omega) = \begin{cases} -j, & 0 < \omega < \pi \\ +j, & -\pi < \omega < 0, \end{cases} \quad (1.3.16)$$

in which case the coefficients b_m are designed to give

$$R(\omega) \approx \begin{cases} -1, & 0 < \omega < \pi \\ +1, & -\pi < \omega < 0, \end{cases} \quad (1.3.17)$$

and there is, of course, a delay of $M/2$.

EXAMPLE
Differentiator

The simplest discrete-time approximation to a continuous-time differentiator is the first-difference operation

$$y(n) = x(n) - x(n - 1)$$

corresponding to the causal first-order type-IV filter

$$h(n) = \delta(n) - \delta(n - 1).$$

The system function is thus

$$H(z) = 1 - z^{-1}$$

which has a single zero at $z = 1$, as expected for conjugate-odd symmetry. The frequency response is

$$\begin{aligned} H'(\omega) &= 1 - e^{-j\omega} \\ &= e^{-j\omega/2}[e^{j\omega/2} - e^{-j\omega/2}] \\ &= 2je^{-j\omega/2} \sin(\omega/2). \end{aligned}$$

Hence, the filter has a linear-plus-90° phase response, as expected, with a group delay of $1/2$. The real function $R(\omega)$ is

$$R(\omega) = 2 \sin(\omega/2)$$

which approximates the desired response in (1.3.15) well for $\omega < \pi/3$, but not for frequencies above that value.

As a final point concerning real FIR networks with even or odd symmetry in the filter coefficients, we note that these networks can be implemented with only $[(M/2) + 1]_{int}$ multipliers. This results from writing $H(z)$ as

$$H(z) = b_0(1 \pm z^{-M}) + b_1(z^{-1} \pm z^{-M+1}) + \dots + b_{M/2}z^{-M/2}$$

for M even, and likewise for M odd without the last term. The corresponding direct-form network is shown in figure 1.13.

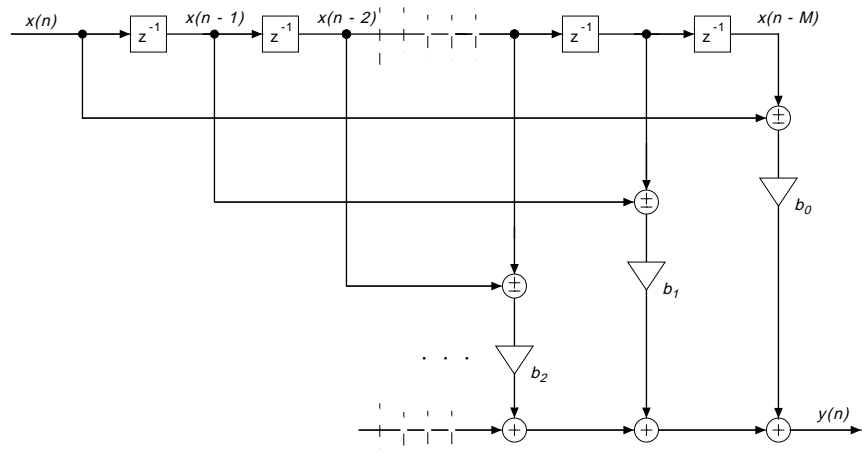


Figure 1.13: Transversal structure with about half the multipliers for linear-phase FIR filters.

MATLAB Exercise No. 8 - Linear-Phase FIR Filters

Generate the following type-I, -II, -III, and -IV linear-phase FIR filters (use help `remez`):

```

h1 = remez(16,[0 0.2 0.3 0.5 0.6 1],[1 1 0 0 1 1]);
h2 = remez(9,[0 0.2 0.5 1],[1 1 0 0]);
h3 = remez(12,[0.1 0.9],[1 1],'hilbert');
h4 = remez(9,[0 0.8],[0 0.8],'differentiator');

```

Plot the corresponding impulse responses and pole/zero diagrams, and compare them with figures 1.11 and 1.12. Also plot the associated magnitude and (unwrapped) phase responses.

Now try the highpass design

```

h5 = remez(9,[0 0.2 0.5 1],[0 0 1 1]);

```

Since this filter is highpass and odd-order, one would expect a zero at $z = 1$, that is, a type-IV design. However, `remez.m` increases the order by one to produce an even-order type-II design. To circumvent this problem and force the desired type-IV design, we can first generate a lowpass filter with the frequency-reversed specification

```
h6 = remez(9,[0 0.5 0.8 1],[1 1 0 0]);
```

and then convert this to a highpass filter via the transformation $H_7(z) = H_6(-z)$, i.e.,

```
n = [0:9];
h7 = (-1).^n.*h6;
```

Plot the pole-zero diagrams and the impulse and magnitude responses for $H_6(z)$ and $H_7(z)$.

1.4 Special Discrete-Time Networks

In addition to linear-phase filters, there are many other special discrete-time networks with interesting and useful properties. Those to be considered here are the allpass filter, the comb filter, and complementary filters.

Allpass Filters

An *allpass* filter has a magnitude response that is unity for all frequencies, i.e.,

$$|H'(\omega)| = 1, \quad \text{for all } \omega. \quad (1.4.1)$$

Such filters are useful for phase equalization of IIR designs and low-sensitivity IIR implementations, and they also play a central role in discrete-time spectral transformations (see section 8.4). The system function of an allpass filter is of the form

$$\begin{aligned} H(z) &= \frac{\sum_{k=0}^N a_k z^{-N+k}}{\sum_{k=0}^N a_k z^{-k}} = \frac{z^{-N} + a_1 z^{-N+1} + \dots + a_N}{1 + a_1 z^{-1} + \dots + a_N z^{-N}} \\ &= \prod_{i=1}^L \frac{z^{-2} + \alpha_{1i} z^{-1} + \alpha_{2i}}{1 + \alpha_{1i} z^{-1} + \alpha_{2i} z^{-2}}, \end{aligned} \quad (1.4.2)$$

where all coefficients are real. Hence, the numerator and denominator coefficients are the same except that their order is reversed in both the direct and cascade forms. To see that (1.4.2) implies (1.4.1), we rewrite (1.4.2) as

$$H(z) = \frac{z^{-N} \sum_{k=0}^N a_k z^k}{\sum_{k=0}^N a_k z^{-k}} = z^{-N} \frac{D(z^{-1})}{D(z)}. \quad (1.4.3)$$

It follows immediately that

$$|H'(\omega)| = \left| \frac{D'(-\omega)}{D'(\omega)} \right| = 1$$

because $|D'(\omega)|$ is an even function if $D(z)$ has real coefficients. From (1.4.3) we also note that the zeros of $H(z)$ are the reciprocals of its poles. A typical pole/zero diagram of an allpass filter is illustrated in figure 1.14.

A cascade-form allpass section having three multipliers is shown in figure 1.15. Cascade-form networks with only two multipliers per section can also be generated [?].

Note that the structure of figure 1.15 inherently satisfies the allpass condition in (1.4.2), even with coefficient quantization.

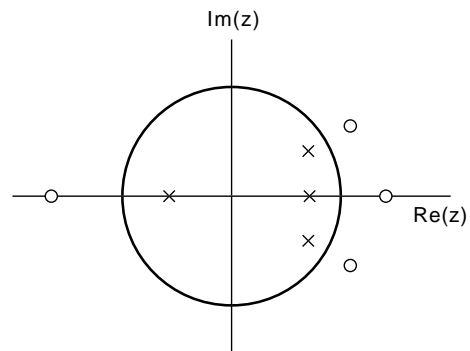


Figure 1.14: Sample allpass pole/zero diagram showing reciprocal pole/zero pairs.

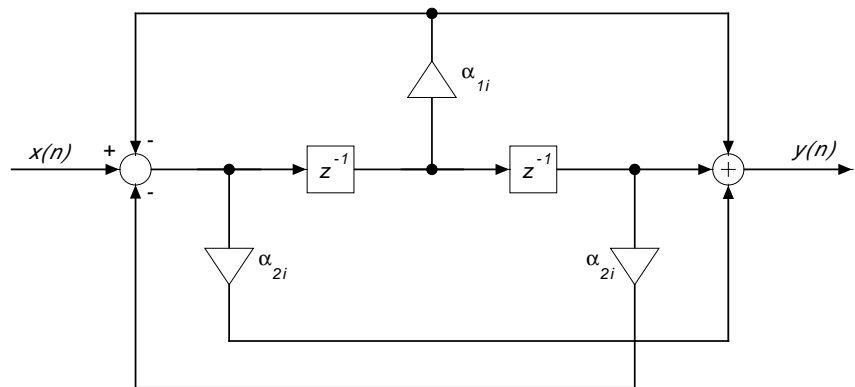


Figure 1.15: Second-order cascade-form allpass section.

Many other structures, including the lattice structure (output $\hat{y}(n)$ in figure 10.11 and those in [?]), are also inherently allpass. Such allpass structures are said to be *structurally lossless* or *structurally passive*.

Comb Filters

Given an arbitrary system function $H(z)$, consider the response of a filter with the system function $H(z^k)$. Since $H'(\omega)$ is periodic with period 2π , $H'(k\omega)$ must be periodic with period $2\pi/k$. Hence, the frequency response corresponding to $H(z^k)$ is periodic within the Nyquist interval $0 \leq \omega \leq \pi$. Such filters are called *comb filters* and have various applications, including the suppression of *clutter* from fixed objects in moving-target-indicator (MTI) radars, the suppression of cross-rate interference in Loran navigation systems, and pitch detection in speech coders. The comb filter is also a useful concept for analyzing certain algorithms such as the Arithmetic Fourier Transform (AFT) [?].

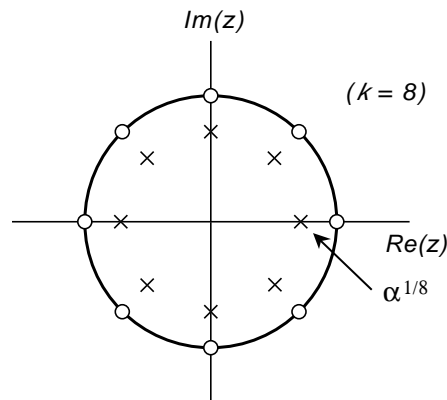


Figure 1.16: Sample pole/zero diagram for a comb filter.

As an example of comb filters, we will transform the highpass function

$$H(z) = \frac{1 - z^{-1}}{1 - \alpha z^{-1}}$$

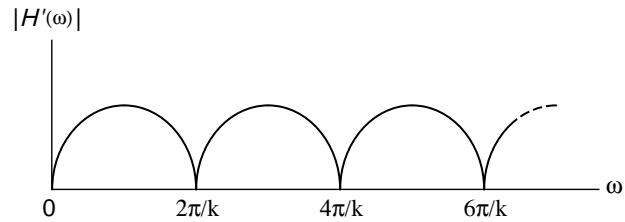


Figure 1.17: Sample comb-filter magnitude response.

into a mult notch comb filter by substituting z^k for z . The system function $H_k(z)$ for the comb filter is then

$$H_k(z) = H(z^k) = \frac{1 - z^{-k}}{1 - \alpha z^{-k}},$$

which has the pole/zero diagram shown in figure 1.16 (for $k = 8$). The corresponding frequency response is sketched in figure 1.17, and we see that the frequency $2\pi/k$ and all its harmonics will be rejected by this filter (as well as $\omega = 0$, or dc). An implementation of this filter is diagrammed in figure 1.18.

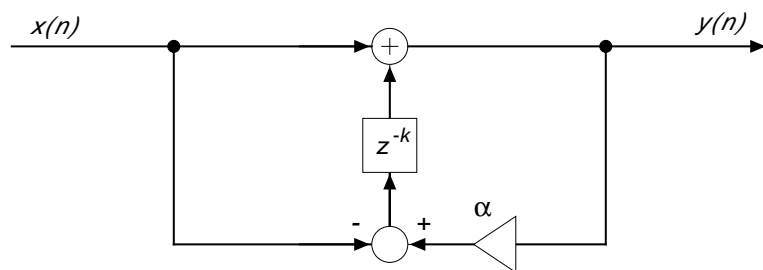


Figure 1.18: Comb-filter implementation for figures 1.16 and 1.17.

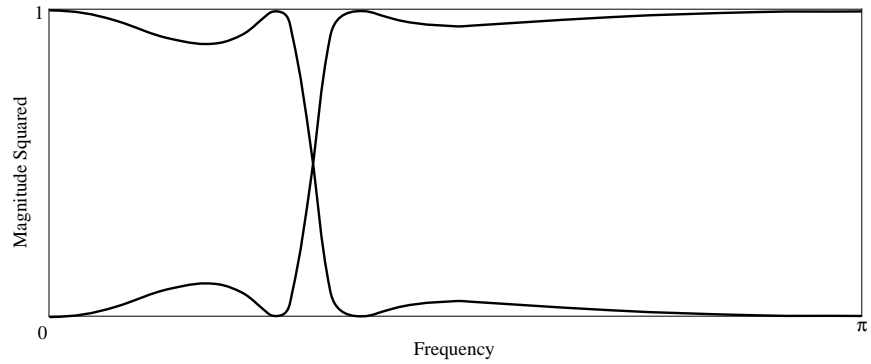


Figure 1.19: Power-complementary third-order elliptic lowpass and highpass responses.

Complementary Filters

A pair of filters $H_1(z)$ and $H_2(z)$ (either FIR or IIR) is said to be *power-complementary* if

$$|H_1'(\omega)|^2 + |H_2'(\omega)|^2 = 1 \quad (1.4.4)$$

for all ω . For filters with real-valued coefficients, this is equivalent to the z -transform requirement that

$$H_1(z)H_1(z^{-1}) + H_2(z)H_2(z^{-1}) = 1. \quad (1.4.5)$$

For example, if $H_1(z)$ is lowpass, then $H_2(z)$ is highpass as illustrated in figure 1.19, while if $H_1(z)$ is bandstop, then $H_2(z)$ is bandpass. Note that in order for $H_1(z)$ and $H_2(z)$ to satisfy (1.4.4) and (1.4.5), they must be *bounded real*, that is,

$$|H_i'(\omega)| \leq 1. \quad (1.4.6)$$

Given an N th-order bounded-real filter

$$H_1(z) = \frac{P(z)}{D(z)} \quad (1.4.7)$$

it is always possible to find the corresponding power complement

$$H_2(z) = \frac{Q(z)}{D(z)} \quad (1.4.8)$$

because, from (1.4.5),

$$P(z)P(z^{-1}) + Q(z)Q(z^{-1}) = D(z)D(z^{-1}), \quad (1.4.9)$$

and thus $Q(z)$ can be obtained from $H_1(z)$ as a spectral factor of

$$Q(z)Q(z^{-1}) = D(z)D(z^{-1}) - P(z)P(z^{-1}). \quad (1.4.10)$$

That is, rooting the $2N$ th-order zero-phase polynomial $Q(z)Q(z^{-1})$, we can separate the zeros into reciprocal pairs z_k and z_k^{-1} , $k = 1, 2, \dots, N$, and then select the $\{z_k\}$ for $Q(z)$, leaving $\{z_k^{-1}\}$ for $Q(z^{-1})$. Of course, if the filters are FIR, then $D(z) = 1$.

In the case of classical IIR filters (Butterworth, Chebyshev, and elliptic—see chapter 8), $P(z)$ and $Q(z)$ have all their zeros on the unit circle (implying that $Q(z)Q(z^{-1})$ has double zeros on the unit circle). Hence, $P(z)$ and $Q(z)$ are linear-phase polynomials with even or odd symmetry. In particular, for a lowpass or bandstop filter $H_1(z)$, we have $H_1(1) \neq 0$, and thus $P(z)$ has even symmetry. If $H_1(1) = 1$, then the complementary highpass or bandpass filter $H_2(z)$ must satisfy $H_2(1) = 0$, and $Q(z)$ has at least one zero at $z = 1$. If N is odd, the number of zeros of $Q(z)$ at $z = 1$ is odd, and thus $Q(z)$ has odd symmetry. Therefore, for $H_1(1) = 1$ and N odd, $P(z)$ is type II and $Q(z)$ is type IV.

In this important special case, it can be shown [?] that $H_1(z)$ and $H_2(z)$ can be realized as parallel combinations of two stable allpass filters $A_1(z)$ and $A_2(z)$ with real-valued coefficients as shown in figure 1.20, *i.e.*,

$$\begin{aligned} H_1(z) &= \frac{1}{2}[A_1(z) + A_2(z)], \\ H_2(z) &= \frac{1}{2}[A_1(z) - A_2(z)], \end{aligned} \quad (1.4.11)$$

from which we see that the required allpass filters are simply

$$\begin{aligned} A_1(z) &= H_1(z) + H_2(z), \\ A_2(z) &= H_1(z) - H_2(z). \end{aligned} \quad (1.4.12)$$

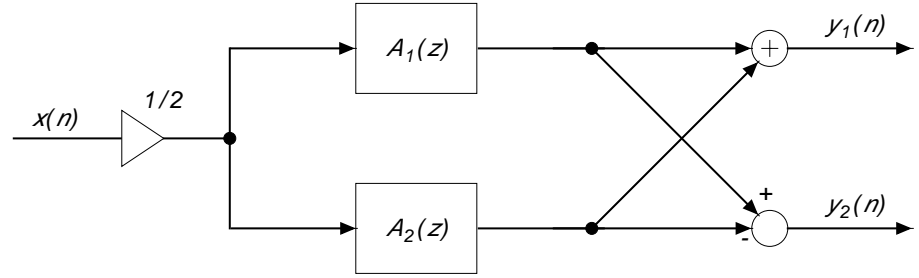


Figure 1.20: Allpass realization of a doubly-complementary filter pair.

Since $H_1(z) + H_2(z)$ equals the allpass filter $A_1(z)$, we say that $H_1(z)$ and $H_2(z)$ are *complementary with respect to $A_1(z)$* , and since they are also power-complementary, they are said to form a *doubly-complementary pair*. If the implementations $A_1(z)$ and $A_2(z)$ are structurally lossless (i.e., constrained to be allpass even with coefficient quantization), then $H_1(z)$ and $H_2(z)$ must be bounded real, in which case the implementation of figure 1.20 is *structurally bounded*. As discussed in chapter 11, this implies very low sensitivity to coefficient quantization in the passband.

The allpass filters $A_1(z)$ and $A_2(z)$ have orders N_1 , and N_2 , respectively, with $N_1 + N_2 = N$. That is, from (1.4.12),

$$\begin{aligned} A_1(z) &= \frac{P(z) + Q(z)}{D(z)} = \frac{z^{-N_1} D_1(z^{-1})}{D_1(z)} \\ A_2(z) &= \frac{P(z) - Q(z)}{D(z)} = \frac{z^{-N_2} D_2(z^{-1})}{D_2(z)} \end{aligned} \quad (1.4.13)$$

with $D(z) = D_1(z)D_2(z)$. Specifically, N_2 zeros of $P(z) + Q(z)$ cancel N_2 poles of $1/D(z)$ to yield $A_1(z)$, while N_1 zeros of $P(z) - Q(z)$ cancel the other N_1 poles of $1/D(z)$ to yield $A_2(z)$.

If the filter order N is even, $Q(z)$ has even symmetry, and the simple implementation of figure 1.20 is not applicable. However, a closely related implementation based on a complex allpass filter has been developed [?].

EXAMPLE

The only first-order IIR lowpass filter satisfying the requirements $H_1(1) = 1$ and $H_1(-1) = 0$ is

$$H_1(z) = \frac{\frac{1}{2}(1-a)(1+z^{-1})}{1-az^{-1}}, \quad (1.4.14)$$

and likewise, for $H_2(1) = 0$ and $H_2(-1) = 1$, we have the highpass filter

$$H_2(z) = \frac{\frac{1}{2}(1+a)(1-z^{-1})}{1-az^{-1}}. \quad (1.4.15)$$

One can readily verify that $H_1(z)$ and $H_2(z)$ are power-complementary. Therefore, since

$$P(z) + Q(z) = 1 - az^{-1} = D(z)$$

and

$$P(z) - Q(z) = z^{-1} - a,$$

we can realize $H_1(z)$ and $H_2(z)$ in the form of figure 5.20 with the allpass filters

$$A_1(z) = 1$$

and

$$A_2(z) = \frac{z^{-1} - a}{1 - az^{-1}}.$$

1.5 Relationships between Magnitude and Phase Responses

As discussed in section 4.3, the locations of poles and zeros influence both the magnitude and phase responses of a system. In this section, we shall study these important magnitude and phase relationships in more detail.

1.5.1 Minimum-phase Systems

Consider the frequency response $H_1(e^{j\omega})$ of a system with just one zero located at a_1 , where $a_1 = r_1 e^{j\theta_1}$, $r_1 < 1$, i.e. ,

$$H_1(e^{j\omega}) = 1 - a_1 e^{-j\omega}. \quad (1.5.1)$$

Taking the natural logarithm of both sides and using the power series expansion for $\ln(1 - x)$, we have

$$\begin{aligned} \ln(H_1(e^{j\omega})) &= \ln(1 - a_1 e^{-j\omega}) \\ &= \sum_{n=1}^{\infty} \frac{-1}{n} a_1^n e^{-jn\omega} \\ &= \underbrace{\sum_{n=1}^{\infty} \frac{-r_1^n \cos(n\omega - n\theta_1)}{n}}_{\alpha_1(\omega)} + j \underbrace{\sum_{n=1}^{\infty} \frac{r_1^n \sin(n\omega - n\theta_1)}{n}}_{\hat{\alpha}_1(\omega)} \\ &= \alpha_1(\omega) + j\hat{\alpha}_1(\omega). \end{aligned}$$

Thus the frequency response $H_1(e^{j\omega})$ may be expressed in terms of the real functions $\alpha_1(\omega)$ and $\hat{\alpha}_1(\omega)$ as

$$H_1(e^{j\omega}) = e^{\alpha_1(\omega) + j\hat{\alpha}_1(\omega)}. \quad (1.5.2)$$

Note that the log-magnitude $\alpha_1(\omega)$ and the phase response $\hat{\alpha}_1(\omega)$ of this system are related by the Hilbert transform because $\sin n\omega$ is the Hilbert transform of $\cos n\omega$.

Now consider a general M th-order FIR system with all its zeros inside the unit circle. Its system function (within a scale factor) may be written as a product of first-order factors as follows :

$$H(z) = \prod_{k=1}^M (1 - a_k z^{-1}). \quad (1.5.3)$$

Since each factor $(1 - a_k z^{-1})$ will contribute a term of the form

$$e^{\alpha_k(\omega) + j\hat{\alpha}_k(\omega)}$$

to the frequency response, $H(e^{j\omega})$ is given by

$$H(e^{j\omega}) = e^{\alpha(\omega) + j\hat{\alpha}(\omega)} \quad (1.5.4)$$

where

$$\begin{aligned}\alpha(\omega) &= \sum_{k=1}^M \alpha_k(\omega), \\ \hat{\alpha}(\omega) &= \sum_{k=1}^M \hat{\alpha}_k(\omega).\end{aligned}$$

Again note that the log-magnitude and phase responses of the system are related by the Hilbert transform. Likewise, if a system has a pole located inside the unit circle at a_k , its contribution to the frequency response is $(1 - a_k e^{-j\omega})^{-1}$. Since $\ln(1 - a_k e^{-j\omega})^{-1} = -\alpha_k(\omega) - \hat{\alpha}_k(\omega)$, the log-magnitude and phase still obey the Hilbert transform property. Therefore, for FIR systems with all zeros inside the unit circle and stable IIR systems with poles and zeros inside the unit circle, the phase and magnitude responses all have the same form as in (1.5.4). Such systems are called *minimum-phase* systems for reasons that we will demonstrate. Minimum-phase systems are invertible.

1.5.2 Maximum-phase Systems

Consider again a first-order system with a zero outside the unit circle at $1/a_1^*$ i.e., $H_2(z) = z^{-1} - a_1^*$, where a_1 is defined as before in (1.5.1). The logarithm of the frequency response of this system is

$$\begin{aligned}\ln(H_2(e^{j\omega})) &= \ln(e^{-j\omega} - a_1^*) \\ &= -j\omega + \ln(1 - a_1^* e^{j\omega}) \\ &= -j\omega + \alpha_1(\omega) - j\hat{\alpha}_1(\omega).\end{aligned}$$

The last step in the previous equation follows from the fact that $\ln(1 - a_1^* e^{j\omega}) = \ln(H_1^*(e^{j\omega}))$. Thus the frequency response $H_2(e^{j\omega})$ may be expressed as

$$H_2(e^{j\omega}) = e^{\alpha_1(\omega) - j(\hat{\alpha}_1(\omega) + \omega)}. \quad (1.5.5)$$

As expected, the magnitude responses of $H_1(e^{j\omega})$ and $H_2(e^{j\omega})$ are identical. However, the phase response of $H_2(e^{j\omega})$ has an additional linear phase term. Also the non-linear part of the phase function $\angle H_2(e^{j\omega})$ is equal to $-\angle H_1(e^{j\omega})$. This system is *maximum-phase*.

Considering an M th-order maximum-phase system as a cascade of M first-order systems, its frequency response may be expressed as

$$H(e^{j\omega}) = e^{\alpha(\omega) - j\hat{\alpha}(\omega) - jM\omega} \quad (1.5.6)$$

where $\alpha(\omega)$ and $\hat{\alpha}(\omega)$ are defined as before. For a given magnitude response, a maximum-phase system has the largest possible phase lag due to the the linear phase term in its frequency response in (1.5.6). The name “maximum-phase” is derived from this maximum phase-lag property. Note that if $H_1(z)$ and $H_2(z)$ are cascaded together, then the non-linear phase contributions from these two frequency responses cancel each other, resulting in a linear-phase frequency response. Thus the linear-phase contribution of a linear-phase filter actually comes from its maximum-phase part. Zeros on the unit circle will also contribute a linear phase term to the frequency response. Occasionally, maximum-phase systems are defined to include zeros on the unit circle as well.

In purely minimum-phase or maximum-phase systems, the magnitude and phase responses are closely tied to each other, i.e., specification of the magnitude response essentially determines the phase response, and vice-versa. Hence filters with arbitrary magnitude and phase responses can not be realized by purely minimum-phase or maximum-phase systems, in general.

1.5.3 Allpass Systems

Allpass systems have a constant magnitude response and a non-trivial phase response. Consider the first-order allpass system $H_3(z)$ defined using $H_1(z)$ and $H_2(z)$ from the previous subsections as

$$\begin{aligned} H_3(z) &= \frac{H_2(z)}{H_1(z)} \\ &= \frac{z^{-1} - a_1^*}{1 - a_1 z^{-1}}. \end{aligned} \quad (1.5.7)$$

That is, the pole of $H_3(z)$ is located inside the unit circle at a_1 and its corresponding zero is located at the reciprocal conjugate location $1/a_1^*$. Substituting for the frequency responses $H_1(e^{j\omega})$ and $H_2(e^{j\omega})$

from (1.5.2) and (1.5.5), we have

$$\begin{aligned} H_3(e^{j\omega}) &= \frac{e^{\alpha_1(\omega)-j(\hat{\alpha}_1(\omega)+\omega)}}{e^{\alpha_1(\omega)+j\hat{\alpha}_1(\omega)}} \\ &= e^{-j\omega-2j\hat{\alpha}_1(\omega)}. \end{aligned} \quad (1.5.8)$$

Thus the magnitude response of $H_3(z)$ is unity. The *group delay* of $H_3(z)$ is defined as

$$\begin{aligned} \tau_3(\omega) &= -\frac{d}{d\omega} \angle H_3(e^{j\omega}) \\ &= -\frac{d}{d\omega} (-\omega - 2\hat{\alpha}_1(\omega)) \\ &= -\frac{d}{d\omega} \left(-\omega - 2 \sum_{n=1}^{\infty} \frac{r_1^n \sin(n\omega - n\theta_1)}{n} \right) \\ &= 1 + 2 \sum_{n=1}^{\infty} r_1^n \cos(n\omega - n\theta_1) \\ &= 1 + \sum_{n=1}^{\infty} (r_1^n e^{j(n\omega - n\theta_1)} + r_1^n e^{-j(n\omega - n\theta_1)}). \end{aligned}$$

Writing the geometric sums in closed form, we have

$$\begin{aligned} \tau_3(\omega) &= \frac{1}{1 - a_1^* e^{j\omega}} + \frac{1}{1 - a_1 e^{-j\omega}} - 1 \\ &= \frac{1 - r_1^2}{|1 - a_1 e^{-j\omega}|^2}. \end{aligned} \quad (1.5.9)$$

Since $r_1 < 1$, $\tau_3(\omega)$, which equals the negative of the slope of the phase response, is a positive quantity for all ω . This implies that the (unwrapped) phase response of the allpass filter $H_3(z)$ is a monotonically decreasing function in the interval $-\pi < \omega < \pi$. Since a higher-order allpass system can be regarded as a cascade of first-order allpass systems, it follows that the group delay of any order allpass system is positive for all frequencies. Consequently, its phase response monotonically decreases.

1.5.4 Decomposition of Non-Minimum-phase Systems

A minimum-phase system is both causal and stable and has all its zeros and poles inside the unit circle. Consider a stable and causal non-

minimum-phase system $H(z)$. Assume that only one of its zeros is outside the unit circle. We can then write $H(z)$ as the product

$$H(z) = G(z)(z^{-1} - a^*) \quad (1.5.10)$$

where $1/a^*$ is the location of the zero outside the unit circle. $G(z)$ is the part of $H(z)$ which contains all other zeros and poles that are assumed to be inside the unit circle. We shall multiply and divide $H(z)$ by a factor $(1 - az^{-1})$. By grouping the minimum-phase terms together, we can rewrite $H(z)$ as

$$H(z) = \underbrace{G(z)(1 - az^{-1})}_{H_{min}(z)} \underbrace{\frac{(z^{-1} - a^*)}{(1 - az^{-1})}}_{H_{ap}(z)}. \quad (1.5.11)$$

If the non-minimum-phase system has more than one (real or complex) zero outside the unit circle, we can repeat the above process of introducing a pole at the reciprocal complex-conjugate location and cancelling it by a zero at the same location. Then we can separately group the minimum-phase and allpass parts. Thus any non-minimum-phase system may be decomposed as follows:

$$H(z) = H_{min}(z)H_{ap}(z). \quad (1.5.12)$$

We may express the unwrapped or continuous-phase of $H(z)$ as the sum of the phase due to the minimum-phase system and the allpass system, i.e.,

$$\angle H(e^{j\omega}) = \angle H_{min}(e^{j\omega}) + \angle H_{ap}(e^{j\omega}). \quad (1.5.13)$$

Therefore, the group delays of the systems are similarly related as

$$\tau(\omega) = \tau_{min}(\omega) + \tau_{ap}(\omega). \quad (1.5.14)$$

Since we have shown in the previous subsection that $\tau_{ap}(\omega)$ is positive for all ω , it follows that the non-minimum-phase system $H(z)$ has a larger group delay than the corresponding minimum-phase system with the identical magnitude response. This also implies that the phase lag

through the non-minimum-phase system is larger than that of the corresponding minimum-phase system.

Increased phase lag or group delay of non-minimum-phase systems also manifests itself in the magnitude of the impulse response samples of these systems. Specifically, a minimum-phase system tends to have a larger portion of its energy concentrated in its initial impulse response samples (close to $n = 0$) compared to a non-minimum-phase system with identical frequency-response magnitude. We shall demonstrate this for a simple case in the following example.

EXAMPLE

Let $H(z)$ be a causal non-minimum-phase system. Let $H_{min}(z)$ be a minimum phase system with the identical magnitude response. Clearly,

$$\int_{-\pi}^{\pi} |H(e^{j\omega})|^2 d\omega = \int_{-\pi}^{\pi} |H_{min}(e^{j\omega})|^2 d\omega. \quad (1.5.15)$$

Using Parseval's relationship it follows that

$$\sum_{n=0}^{\infty} |h(n)|^2 = \sum_{n=0}^{\infty} |h_{min}(n)|^2 \quad (1.5.16)$$

where $h(n)$ and $h_{min}(n)$ are the corresponding impulse responses. That is, the total energy in the two impulse response sequences are the same. Now, let us consider the partial energy in the first $m + 1$ samples of $h(n)$ and $h_{min}(n)$. For simplicity, assume that $H(z)$ has only one zero outside the unit circle. If we denote the zero outside as $1/a^*$, then we can write $H(z)$ as

$$H(z) = G(z)(z^{-1} - a^*). \quad (1.5.17)$$

All other zeros and poles of $H(z)$ are inside the unit circle and are grouped under the system function $G(z)$. The minimum-phase system $H_{min}(z)$, which has the same magnitude response as $H(z)$, is given by

$$H_{min}(z) = G(z)(1 - az^{-1}). \quad (1.5.18)$$

Now, taking the inverse z-transform of (1.5.17) and (1.5.18), we obtain

$$h(n) = g(n - 1) - a^*g(n) \quad (1.5.19)$$

and

$$h_{min}(n) = g(n) - ag(n-1). \quad (1.5.20)$$

Let $\Delta E(m)$ denote the difference in energy in the first $m+1$ samples of the two impulse responses $h(n)$ and $h_{min}(n)$, i.e.,

$$\Delta E(m) = \sum_{n=0}^m (|h_{min}(n)|^2 - |h(n)|^2). \quad (1.5.21)$$

Substituting for the impulse responses from (1.5.19) and (1.5.20) and using the fact that $G(z)$ is a causal system and $|h(n)|^2 = h(n)h^*(n)$, etc., we find that

$$\begin{aligned} \Delta E(m) &= \sum_{n=0}^m (|g(n)|^2(1-|a|)^2 - |g(n-1)|^2(1-|a|)^2) \\ &= |g(m)|^2(1-|a|^2). \end{aligned} \quad (1.5.22)$$

Since $|a|^2 < 1$, (1.5.21) then implies that

$$\sum_{n=0}^m |h_{min}(n)|^2 \geq \sum_{n=0}^m |h(n)|^2. \quad (1.5.23)$$

That is, the energy in the first $m+1$ impulse response samples of $H_{min}(z)$ is greater than or equal to that in the first $m+1$ impulse response samples of $H(z)$. But as m approaches infinity in Eq.(1.5.22) the energy difference $\Delta E(m)$ tends to zero because $|g(m)|$ tends to zero. Although the above expression is derived for the case of a $H(z)$ with only one zero outside the unit circle, the inequality in (1.5.23) holds for a general $H(z)$ with multiple zeros outside the unit circle and its corresponding minimum-phase system $H_{min}(z)$ as well (See Problem 5.29). The following numerical example further illustrates the properties of the minimum/non-minimum/maximum-phase systems discussed in this section.

EXAMPLE

Figures 1.21(a), (b), (c) and (d) show the pole-zero plots for four different FIR filter transfer functions $H_1(z)$, $H_2(z)$, $H_3(z)$, and $H_4(z)$, respectively, where

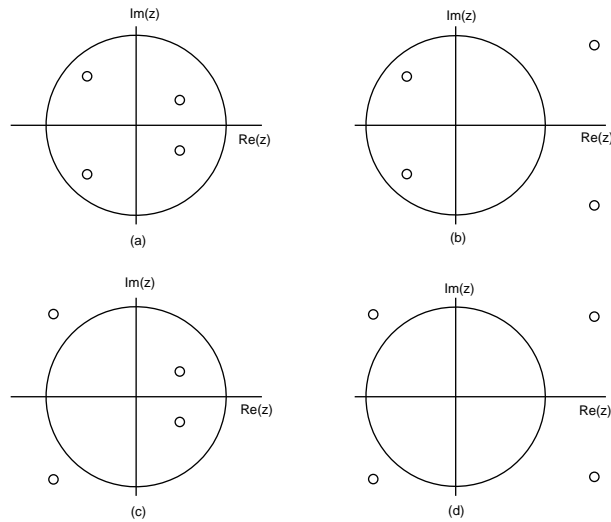


Figure 1.21: Pole-zero plots of the four sample FIR filters.

$$\begin{aligned}
 H_1(z) &= (1 - 0.56e^{j\pi/6}z^{-1})(1 - 0.56e^{-j\pi/6}z^{-1}) \times \\
 &\quad (1 - 0.77e^{j3\pi/4}z^{-1})(1 - 0.77e^{-j3\pi/4}z^{-1}) \\
 H_2(z) &= (z^{-1} - 0.56e^{-j\pi/6})(z^{-1} - 0.56e^{j\pi/6}) \times \\
 &\quad (1 - 0.77e^{j3\pi/4}z^{-1})(1 - 0.77e^{-j3\pi/4}z^{-1}) \\
 H_3(z) &= (1 - 0.56e^{j\pi/6}z^{-1})(1 - 0.56e^{-j\pi/6}z^{-1}) \times \\
 &\quad (z^{-1} - 0.77e^{-j3\pi/4})(z^{-1} - 0.77e^{j3\pi/4}) \\
 H_4(z) &= (z^{-1} - 0.56e^{-j\pi/6})(z^{-1} - 0.56e^{j\pi/6}) \times \\
 &\quad (z^{-1} - 0.77e^{-j\pi/6})(z^{-1} - 0.77e^{j\pi/6}).
 \end{aligned}$$

$H_1(z)$ is a minimum-phase filter and $H_4(z)$ is maximum-phase. The non-minimum-phase filter $H_2(z)$ is obtained from $H_1(z)$ by flipping two of its zeros on the right half of the z -plane to outside the unit circle. Similarly $H_3(z)$ is obtained from $H_1(z)$ by flipping the other two zeros outside the circle. If we flip all zeros of $H_1(z)$ outside the circle, we have $H_4(z)$.

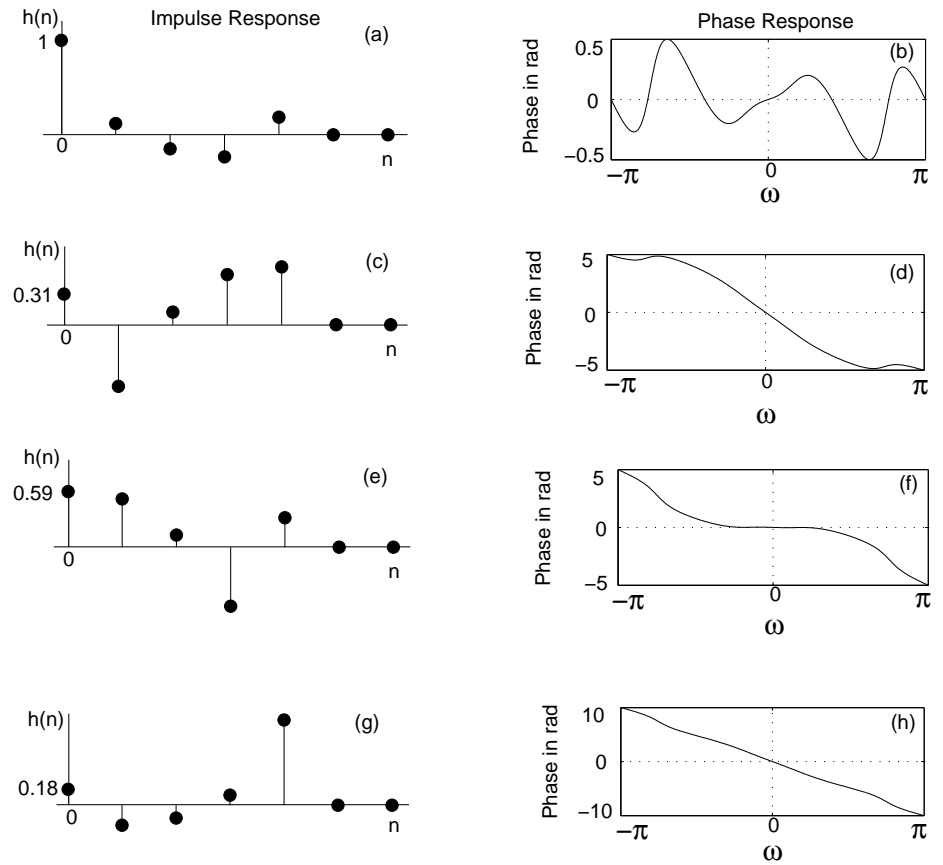


Figure 1.22: Impulse responses and unwrapped phase responses of the four sample FIR filters.

The corresponding impulse responses and unwrapped phase responses for the four filters are shown in figure 1.22. Note that, as expected, all four filters have identical magnitude responses (not shown). Also notice that the minimum-phase filter $H_1(z)$ has the smallest phase lag (figure 1.22 (b)) whereas the maximum-phase filter has the largest (figure 1.22 (h)). Note that the non-minimum phase filter $H_2(z)$, for example, may be decomposed into minimum-phase and allpass factors as follows:

$$H_2(z) = H_1(z) \left\{ \frac{(z^{-1} - 0.56e^{-j(\pi/6)})(z^{-1} - 0.56e^{j(\pi/6)})}{(1 - 0.56e^{-j(\pi/6)}z^{-1})(1 - 0.56e^{j(\pi/6)}z^{-1})} \right\}.$$

Observe (see figures 1.22 (a), (c), (e), and (g)) that for the minimum-phase system $H_1(z)$, a significant portion of the total energy in the impulse response samples is concentrated in the first few samples close to the origin $n = 0$. On the other hand, for the maximum-phase system $H_2(z)$ the energy is concentrated at the tail end. The same point is made in figure 1.23 where the partial energy $E(m)$ in the first $m + 1$ samples of the impulse response is plotted as a function of m for each system. Also note that for these FIR filters, $h_4(n) = h_1(M - n)$ and $h_3(n) = h_2(M - n)$, where the order M equals 4.

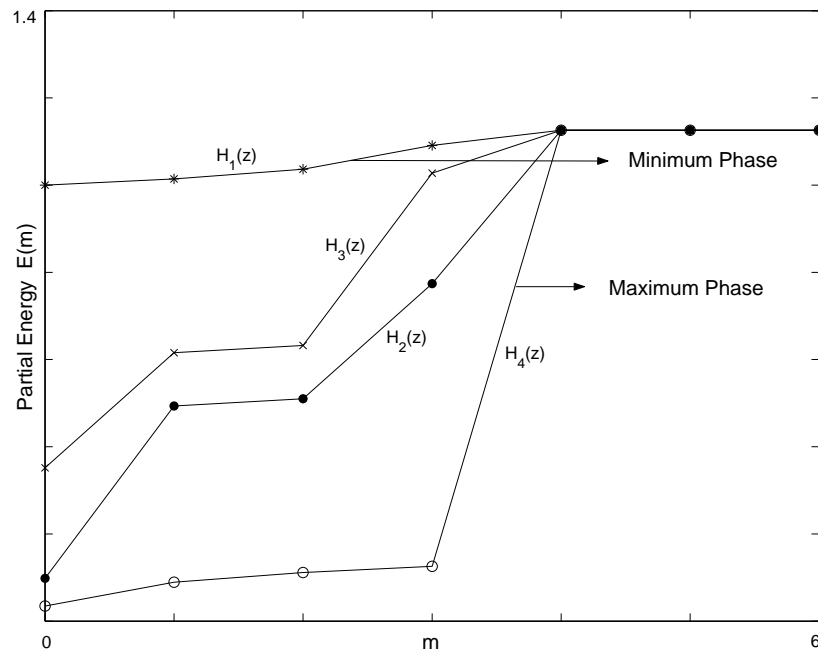
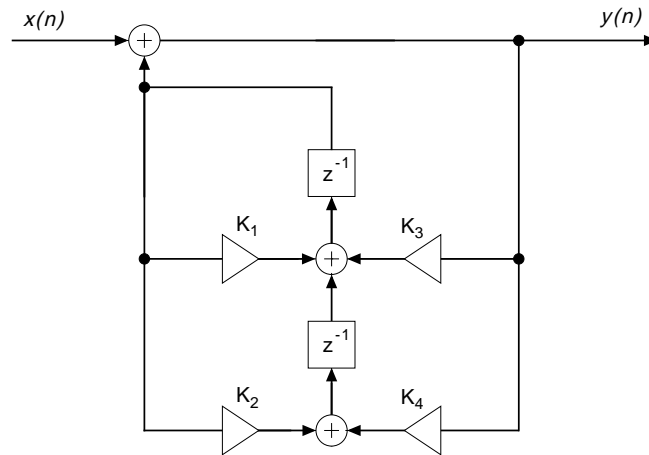


Figure 1.23: Partial energies of the four sample FIR filters.

Problems

5.1 Derive equation (1.1.3) for the system function $H(z)$ of a feedback network by relating $X(z)$, $Y(z)$, and $W(z)$ in figure 1.1.

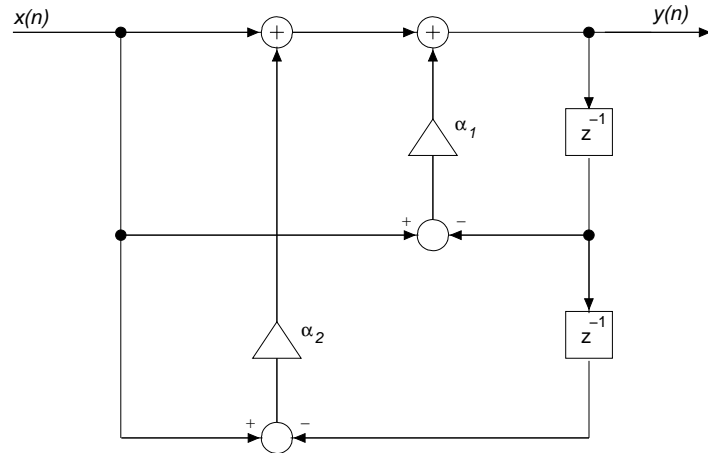
5.2 a. Find $H(z)$ for the network in the figure below. (*Hint*: Identify the feedback network $G(z)$.)



- b. What conditions on the parameters K_i ensure stability?
- c. Draw the transpose network.
- d. Give the state matrices \mathbf{A} , \underline{b} , \underline{c}^t , d .
- e. Find $H(z)$ from (d) and check it with (a).
- f. If the fractional parts of all multiplier coefficients are quantized to the same number of bits, is there any advantage to this configuration over the second-order direct-form structure with regard to the accuracy with which $H(z)$ can be realized? Why?

5.3 As a result of a particular design algorithm, the following causal second-order filter was produced:

$$H(z) = \frac{1 + 2z^{-1} + z^{-2}}{1 - 2z^{-1} + 1.33z^{-2}}$$



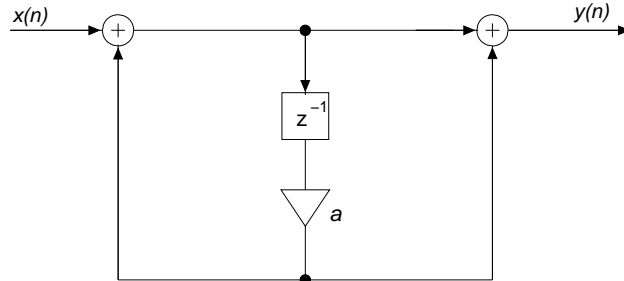
- Is this filter stable?
 - If not, give a causal and stable $H(z)$ having the same magnitude response $|H'(\omega)|$. (*Hint:* Consider the cascade of the unstable system function with an appropriate allpass function.)
 - Sketch $|H'(\omega)|$.
- Show that equation (1.3.7) is required, along with (1.3.6), for the stability of a second-order section.
 - Show that for type-II and -III FIR filters with real coefficients b_m , one zero must lie at $z = -1$. (*Hint:* Look at figure 1.11.)
 - Show that this network has unity gain at dc, i.e., $H(1) = 1$. (*Hint:* Manipulate either the flow graph below or the corresponding difference equations.)
 - Sketch the pole/zero diagram and the magnitude response for the comb filter

$$H(z) = K \frac{1 + z^{-4}}{1 - az^{-4}}.$$

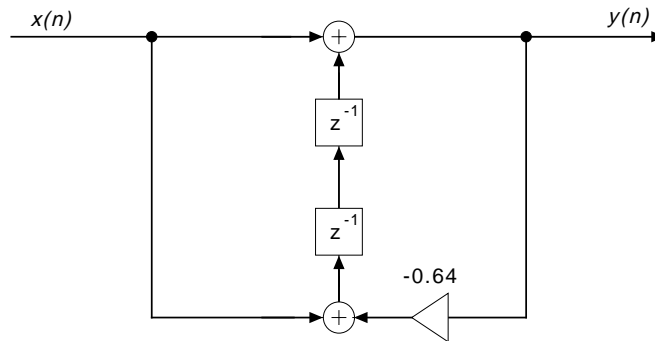
Find K such that the peak gain is unity, and design a structure that incorporates the scaling constant K without an additional

multiplier.

5.8 Find $H(z)$ and $h(n)$ for the network in the figure below.



5.9 Sketch the pole/zero diagram and magnitude response for the network in the figure below.



5.10 Draw direct-form-I and direct-form-II networks for the notch filter in problem 4.10 with $r = 0.95$ and $\theta = 60^\circ$. Which network has potential overflow problems because of large gains to internal nodes?

5.11 Draw a recursive implementation of the simple-averaging filter incorporating a comb filter. (*Hint:* Implement $H(z)$ directly as in (??).) Draw the transpose network. What problems of dc offset or dc accumulation do you see in these networks?

5.12 Find the system function $H_{11}(z)$ from input $x_1(n)$ of figure ?? to the output $s_1(n)$ by feedback analysis. Repeat for $H_{21}(z)$ from the same input to output $s_2(n)$. You may wish to check your answers with those from problem 4.11(c).

5.13 A first-order allpass filter has the system function

$$H(z) = \frac{z^{-1} - a}{1 - az^{-1}}.$$

- Draw form-I and form-II networks for this filter.
- Sketch the phase response $\angle H(\omega)$ of this filter.
- When the coefficient a is quantized to a finite number of bits, its value will be perturbed. Will this perturb the magnitude and/or the phase responses of the filter?

5.14 Find the state matrices \mathbf{A} , \mathbf{b} , \mathbf{c}^t , d for a fourth-order filter in parallel form II. Repeat for cascade form II. (Be careful to include all paths to and from the states.)

5.15 A discrete-time oscillator has the impulse response $h_1(n) = \cos n\omega_0 u(n)$. Draw a network with this impulse response. Repeat for $h_2(n) = \sin n\omega_0 u(n)$. Incorporate both outputs into a single network to produce a *quadrature* oscillator.

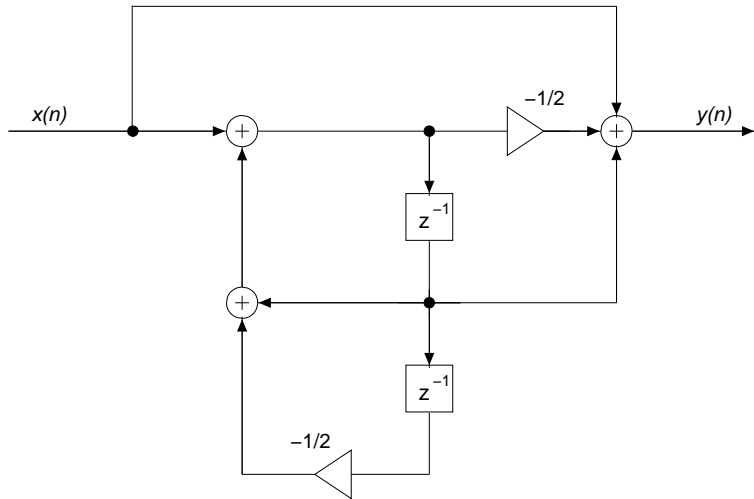
5.16 Draw cascade- and parallel-form-I networks for the following filter using first-order sections:

$$H(z) = \frac{0.7(1 - z^{-2})}{1 - 0.3z^{-1} - 0.4z^{-2}}.$$

Compare the number of multipliers in the two networks.

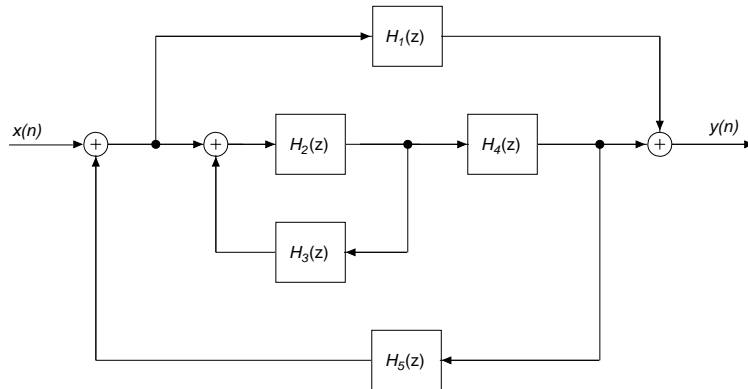
5.17 Sketch the magnitude responses of the four FIR filters in figure 1.12 assuming that each reciprocal pair of zeros implies a dip in the response. Assume also that the filters are *equiripple*, i.e., that the passband ripples are of equal amplitude, and likewise for the stopband, if applicable.

5.18 a. Find $H(z)$ for the network shown.



- b. Sketch the pole/zero diagram.
- c. Sketch the magnitude response $|H'(\omega)|$.
- d. Draw the equivalent direct-form-II network.
- e. Find the state matrices \mathbf{A} , \mathbf{b} , \mathbf{c}^t , d .
- f. Draw the network in state-space form (see figure 4.11).

5.19 Find the overall system function $H(z)$ for the interconnection of subsystems shown.



5.20 A North American and international standard has been established by ANSI and CCITT for digital telephone transmission at 32 kilobits/sec using adaptive differential pulse-code modulation (ADPCM). The ADPCM encoder at the transmitter can be diagrammed as shown below. The adaptive predictor generates a *prediction* $\hat{x}(n)$ of the input signal $x(n)$, and the difference signal $d(n)$ is quantized by an adaptive quantizer Q to produce the encoder output $y(n)$. The decoder at the receiver corresponds to the inverse of the encoder and produces the recovered signal $r(n)$, which, in the absence of the quantization and transmission errors, would equal the original signal $x(n)$. Neglecting the time-varying nature of the adaptive filters $A(z)$ and $B(z)$, their system functions are given by

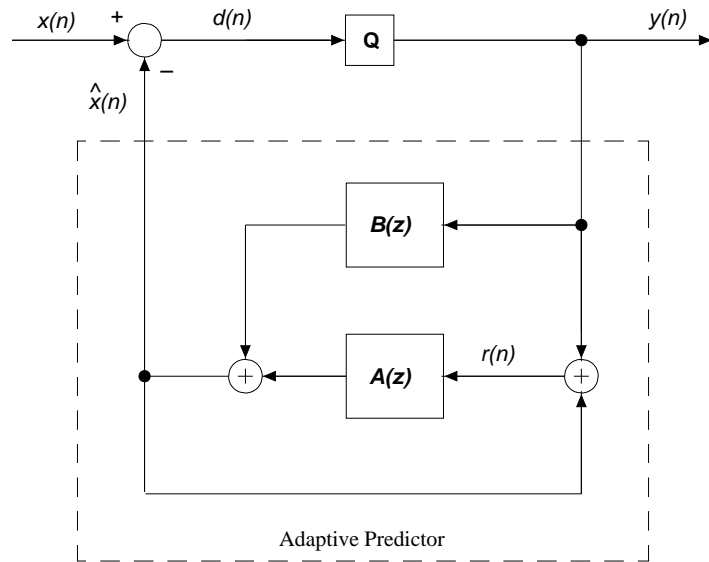
$$A(z) = a_1z^{-1} + a_2z^{-2}$$

and

$$B(z) = b_1z^{-1} + b_2z^{-2} + \dots + b_6z^{-6}$$

We will also neglect the quantizer Q in the following analysis.

- Find the encoder system function $H_e(z)$ from $x(n)$ to $y(n)$.
- Show that the signal $r(n)$ in the encoder equals $x(n)$, i.e., that



the system function $H_r(z)$ from $x(n)$ to $r(n)$ is unity.

c. Diagram a decoder network $H_d(z)$ with input $y(n)$ and output $r(n)$, such that $H_e(z)H_d(z) = 1$.

d. How many (nonzero) poles and zeros does the encoder have? The decoder?

e. Why is it necessary for the encoder to be minimum-phase?

5.21 Consider the FIR technique of *averaging by 4's and 6's* (see problem 4.3).

a. Draw the corresponding pole/zero diagram.

b. Is the overall filter type I or type II?

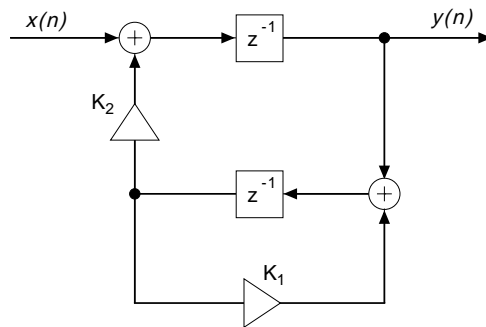
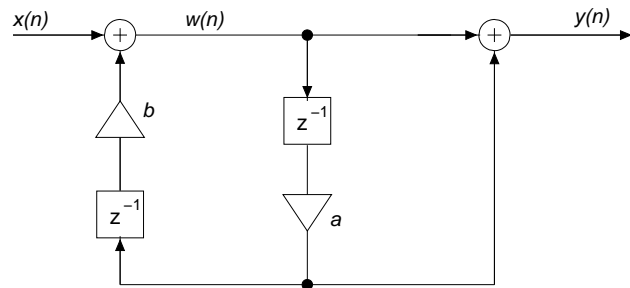
c. Sketch $|H'(\omega)|$. (*Optional*: Plot in dB using MATLAB.)

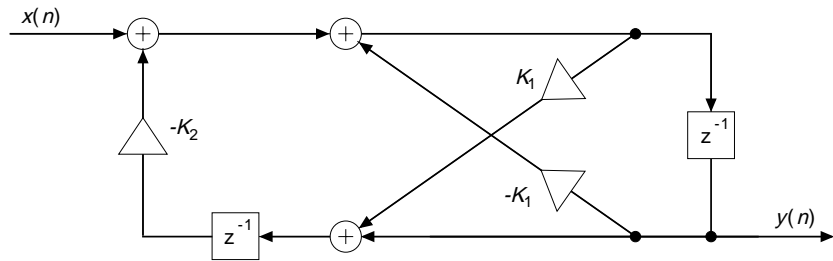
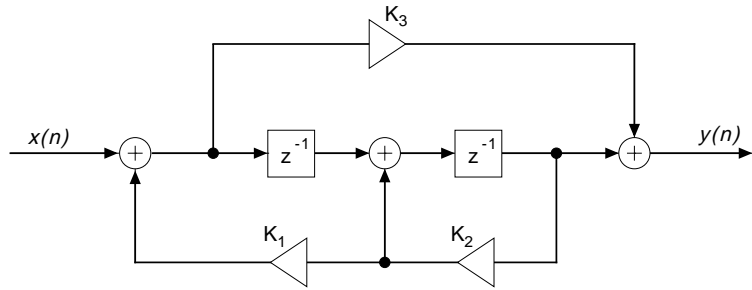
d. Draw the direct-form (transversal) network.

e. Draw the cascade-form network with second-order sections. How many multipliers are required?

5.22 For each of the following second-order systems:

- Find $H(z)$, and state the constraints on the coefficient values for stability.
- Draw the transpose network.
- Find the corresponding state matrices \mathbf{A} , \underline{b} , \underline{c}^t , d .





5.23 For the fourth-order comb filter

$$H(z) = \frac{1}{1 - \frac{1}{4}z^{-4}},$$

- Sketch $H'(\omega)$.
- Draw direct, cascade, and parallel forms with real coefficients.

5.24 For the fourth-order comb filter

$$H(z) = \frac{1 - z^{-4}}{1 - \frac{1}{4}z^{-4}},$$

- Sketch $|H'(\omega)|$.
- Draw the cascade-form-II network with real coefficients.

5.25 For the FIR filter $H(z) = 1 + 1.5z^{-1} - 1.5z^{-2} - z^{-3}$,

- Draw the pole/zero plot. (*Hint*: What type FIR filter is this?)
- Draw an implementation having the minimum number of multipliers.

c. Sketch the magnitude and phase responses. (You should be able to do this without MATLAB, but you may wish to check yourself using MATLAB.)

Repeat the problem for $H(z) = 1 + 1.5z^{-1} + 1.5z^{-2} + z^{-3}$.

- 5.26 Utilizing equation (1.4.5) and MATLAB (conv, roots, etc.), find power-complementary highpass filters for the following FIR low-pass filters, and plot the associated pole/zero diagrams and magnitude-squared responses $|H'_1(\omega)|^2$ and $|H'_2(\omega)|^2$:
- $H_1(z) = \frac{1}{2}(1 + z^{-1})$. (You don't need MATLAB for this one.)
 - $H_1(z) = \frac{1}{3}(1 + z^{-1} + z^{-2})$.
 - $H_1(z) = \frac{1}{6}(1 + z^{-1})(1 + z^{-1} + z^{-2})$.

5.27 Consider a first order allpass system

$$H_{ap}(z) = \frac{z^{-1} - a_1^*}{1 - a_1 z^{-1}}$$

where $a_1 = r_1 e^{j\theta}$, $r_1 < 1$.

a. Show that the phase function of $H_{ap}(z)$ may be expressed as follows (See also the equivalent expression in (1.5.8)):

$$\angle H_{ap}(e^{j\omega}) = -\omega + 2 \tan^{-1} \left\{ \frac{r_1 \sin(\theta - \omega)}{1 - r_1 \cos(\theta - \omega)} \right\}.$$

Obtain the expression for the filter's group delay using the above expression and show that it is always positive. Therefore, as ω is changed monotonically from $-\pi$ to π , $\angle H_{ap}(e^{j\omega})$ changes from $\pi + \phi_1$ to $-\pi + \phi_1$ where ϕ_1 is equal to the $2 \tan^{-1}\{..\}$ term above evaluated at $\omega = \pm\pi$. Thus, the allpass filter's frequency response maps the unit circle onto itself.

b. Show that if $H_{ap}(z)$ has real coefficients (i.e., a_1 is real-valued), then

$$\int_0^\pi \tau_{ap}(\omega) d\omega = \pi,$$

where $\tau_{ap}(\omega)$ is the group delay function of the filter.

c. More generally, show that for an M -th order allpass filter

$$\int_{-\pi}^{\pi} \tau_{ap}(\omega) d\omega = 2M\pi.$$

5.28 Let $A(z)$ denote an M th-order minimum-phase filter with real coefficients :

$$A(z) = a_0 + a_1z^{-1} + a_2z^{-2} + \cdots + a_Mz^{-M}.$$

Let $A(1/z)$ denote the reciprocal polynomial (with roots in reciprocal conjugate locations, i.e., outside the unit circle):

$$A(1/z) = a_0 + a_1z + a_2z^2 + \cdots + a_Mz^M.$$

Define two other polynomials

$$P(z) = [A(z) + z^{-M}A(1/z)]$$

$$Q(z) = [A(z) - z^{-M}A(1/z)].$$

Note that the coefficients of $P(z)$ and $Q(z)$ have even and odd symmetry, respectively.

a. Show that $P(z)$ and $Q(z)$ have all their zeros on the unit circle. (*Hint:* Divide $P(z)$ by $A(z)$ and use the monotonic phase property of allpass filters.)

b. Show that the zero locations of $P(z)$ and $Q(z)$ are interlaced.

In the speech signal analysis literature, the angles corresponding to the $2M$ roots of the two M -th degree polynomials $P(z)$ and $Q(z)$ are called line-spectral-frequencies (LSFs).

5.29 Show that of all the causal systems having the same frequency response magnitude $|H(e^{j\omega})|$, the energy

$$E(m) = \sum_{n=0}^m |h(n)|^2$$

is maximum for all $m \geq 0$ when $h(n)$ is the impulse response of a minimum-phase system, i.e.,

$$\sum_{n=0}^m |h_{min}(n)|^2 \geq \sum_{n=0}^m |h(n)|^2.$$

5.30 Let $H(z)$ be a minimum-phase FIR filter.

$$H(z) = h_0 + h_1 z^{-1} + h_2 z^{-2} + \cdots + h_M z^{-M}.$$

a. Show that

$$\int_{-\pi}^{\pi} \ln |H(e^{j\omega})| d\omega = 2\pi \ln(|h_0|).$$

b. Show that the group delay $\tau(\omega)$ of $H(z)$ with real coefficients must be negative for some values of ω , $0 < \omega < \pi$. (*Hint:* Show that $\int_0^\pi \tau(\omega) d\omega = 0$.)

5.31 Find the minimum-phase filter that has the same magnitude response as the linear-phase filter

$$H(z) = -1 + 4.25z^{-2} - z^{-4}.$$

Check your answer by comparing the gains of both filters at $\omega = 0, \pi/2$, and π .